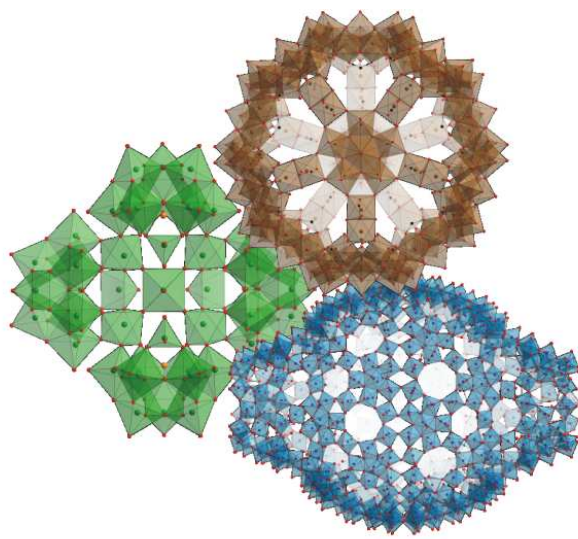


Syntheses and structures of some polyoxomolybdates and polyoxotungstates



-Cumulative dissertation-

Alice Merca

Faculty of Chemistry
University of Bielefeld

June 2005

This thesis is the result of research carried out during the period of November 2001 to May 2005 under the supervision of Prof. Dr. Dr. h. c. mult. Achim Müller, Lehrstuhl für Anorganische Chemie I, Universität Bielefeld.

Referee: Prof. Dr. Dr. h.c. mult. Achim Müller

Second referee: Prof. Dr. Lothar Weber

Acknowledgement

I'm grateful to my supervisor Prof. Dr. Dr. h.c. mult. Achim Müller first of all for offering me the possibility to join his group, for his guidance, as well for the provision of a challenging project.

I am especially grateful to Marc Schmidtman and Dr. Hartmut Bögge for their help with the X-ray diffraction measurements and crystal structure determinations. This thesis would not have been possible without their permanent involvement.

A constant moral support was Karin (K. Lacey) in a place away from home as well as Dr. E. Diemann whose encouraging words were always welcome.

Special thanks regard Soumyajit (Dr. S Roy) for the very fruitful collaborations; Alois (A. Berkle) the best laboratory colleague, for the countless analytical measurements and Liviu (L. Toma) who is a friend from home.

I am grateful to Ms. Gabi Heinze-Brückner for the Infrared and Raman measurements, to Ursula Stuphorn for the UV-Vis measurements and to Ms. Brigitte Michel for the C,H,N analyses .

A number of people have made the challenge of completing doctoral studies in a foreign country possible and enjoyable. My thanks in this regard go to Dr. E. Beckmann, Dr. A. Bell, Dr. B. Botar, M. Bruschi, Dr. D. Fenske, Dr. M. Fricke, M. Harms, E. Krickemeyer, T. Mitra, B. Ostheider, C. Schäffer, Dr. K. Schneider, F. Sousa, A.M. Todea, Dr. R. Tomsa, M. Zimmermann.

Last but not least this thesis would not have been possible without the generous financial support of 'Graduiertenkolleg Strukturbildungsprozesse', University of Bielefeld. I would also like to express my gratitude to Prof. A. Dress and Prof. W.J. Beyn, the directors of the 'GK' for their continuous support.

A final word of gratitude goes to my husband and to my parents.

Contents

1	Introduction	1
1.1	Synopsis	1
1.2	The state of art of the field	2
1.2.1	Polyoxotungstates	2
1.2.2	Polyoxomolybdates	3
1.3	Goals of the project: defining the problem	7
2	Publications	10
2.1	<i>A Small Cavity with Reactive Internal Shell Atoms Spanned by Four {As(W/V)₉}-Type Building Blocks Allows Host Guest Chemistry under Confined Conditions</i> A. Müller, M. T. Pope, A. Merca, H. Bögge, M. Schmidtman, J. van Slageren, M. Dressel, D. G. Kurth <i>Chem. Eur. J.</i> 2005 , accepted.	11
2.2	<i>Trapping Cations in Specific Positions in Tuneable "Artificial Cell" Channels: New Nanochemistry Perspectives</i> A. Müller, S. K. Das, S. Talismanov, S. Roy, E. Beckmann, H. Bögge, M. Schmidtman, A. Merca, A. Berkle, L. Allouche, Y. Zhou, L. Zhang <i>Angew. Chem. Int. Ed.</i> 2003 , <i>42</i> , 5039-5044.	11
2.3	<i>Artificial Cell Decision about Metal Cations Entrance: the "Stable" Aqua Complexes Get Trapped Above the Pores others Slip Out its Water Coat and the Cations Enter</i> A. Müller, A. Merca, H. Bögge, M. Schmidtman, A. Berkle <i>Chem. Commun.</i> 2005 , to be submitted.	12
2.4	<i>Temperature-Dependent Reversible Li⁺ Uptake/Release Equilibrium at Metal-Oxide Nanocontainer-Pores</i> A. Müller, D. Rehder, E.T.K. Haupt, A. Merca, H. Bögge, M. Schmidtman, G. Heinze-Brückner <i>Angew. Chem. Int. Ed.</i> 2004 , <i>43</i> , 4466-4470; Corrigendum: <i>43</i> , 5115.	12

2.5	<i>On the Complex Hedgehog Shaped Cluster Species Containing 368 Mo Atoms: Simple Preparation Method, New Spectral Details and Information About the Unique Formation</i> A. Müller, B. Botar, S. K. Das, H. Bögge, M. Schmidtman, A. Merca <i>Polyhedron</i> 2004 , <i>23</i> , 2381-2385.	13
3	Summary	14
4	Curriculum Vitae	16

Chapter 1

Introduction

1.1 Synopsis

”Just as there is a field of molecular chemistry based on the covalent bond, there is a field of supramolecular chemistry, the chemistry of molecular assemblies and of the intermolecular bond”, wrote J.M Lehn in his book ”Supramolecular Chemistry” in a diagrammatic fashion [1]. Of central importance to supramolecular chemistry is the concept of self assembly, that is: exploiting the tendency of some large systems to self-assemble under suitable conditions. Such processes enable the rapid construction of chemical systems, which display degrees of complexity that would be inaccessible by using conventional sequential synthetic methodologies. A range of intermolecular forces have been investigated, with the goal of building complex molecular assemblies, including: attractive aromatic interactions [2], hydrogen bonding [3], interfacial phenomena [4] and metal-ligand coordination [5]. Many of the resulting supramolecular structures are based on organic components with inorganic components functioning as linking centres.

Polyoxometalate chemistry, the chemistry of the inorganic metal-oxygen cluster anions, uses the advantages of self assembly but based on covalent linking, to synthesise a variety of nano-sized entities which are based on the linking of transferable building blocks, under ”one-pot” conditions. This type of chemistry has already yielded a multitude of compounds containing polyanions which display a fascinating degree of structural and functional variety comparable to that of proteins [6].

Optimal conditions for linking of fragments leading to a large variety of structures are:

- - abundance of a variety of linkable units, i.e. building blocks and the following possibility,
- - of generation of groups (intermediates) with high free enthalpy to drive polymerization or growth processes, e.g. by formation of H_2O ,
- - of an easy structural change in the building units and blocks, of including

hetero elements in the fragments,

- - to form larger groups which can be linked in different ways,
- - to control the structure-forming processes by templates,
- - to generate structural defects in reaction intermediates (e.g. leading to lacunary structures) e.g. by removing building blocks from (large) intermediates due to the presence of appropriate reactants,
- - to localize and delocalize electrons in different ways in order to gain versatility,
- - to control and vary the charge of building parts (e.g. by protonation, electron transfer reactions, or substitution) and to limit growth by the abundance of appropriate terminal ligands,
- - of generating fragments with energetically low-lying unoccupied molecular orbitals. [7]

These conditions can be optimally fulfilled in polyoxometalate systems which possess the relevant variety of structural and electronic versatility. It is not only possible to perform a new type of chemistry with the clusters but also to dissolve them in organic solvents, e.g. after encapsulating them with suitable surfactant molecules, with the option of forming monolayers, thin films and hybrid materials [8]. Furthermore, it is possible to study their aggregation behaviour in solution leading to the formation of novel vesicles [9]. Since this dissertation deals with polyoxotungstates, polyoxomolybdates, consequently a description of their important structural features is necessary.

1.2 The state of art of the field

The basic structural principle for polyoxotungstates and molybdates is the same since the structures are governed by the principle that each metal atom occupies an $\{MO_x\}$ coordination polyhedron, in which the metal atom is displaced, as a result of M-O π bonding, toward those polyhedral vertices that form the surface of the structure. However, a more detailed view of this fascinating area of chemistry shows striking differences for these compound types also with respect to the very large cluster systems [10].

1.2.1 Polyoxotungstates

In contrast to the molybdate species, the structures of very large polytungstate anions may practically all be represented in terms of subunits based on lacunary fragments of the *Keggin* anion or its isomers. This can, in principle, be attributed to the high stability of the related species, which is probably due to the existence of extremely weak but not negligible W-W interactions in the $\{W_3\}$ triangles [11].

Keggin - isomers

The structure of the "basic" *Keggin* anion has overall T_d symmetry and is based on a central XO_4 tetrahedron surrounded by twelve $\{WO_6\}$ octahedra arranged in four groups of three edge-shared octahedra, $\{W_3O_{13}\}$. These $\{W_3O_{13}\}$ groups are linked by shared corners to each other and to the central XO_4 tetrahedron. The *Keggin* structure exists in five different isomers. The most common is the α -isomer, described above. The other isomers of the *Keggin* structure involve the rotation by 60° of one, two, three and all four $\{W_3O_{13}\}$ triplets. In this way the β -(C_{3v}), γ -(C_{2v}), δ -(C_{3v}) and ϵ -isomer (T_d) are formed[12, 13, 14].

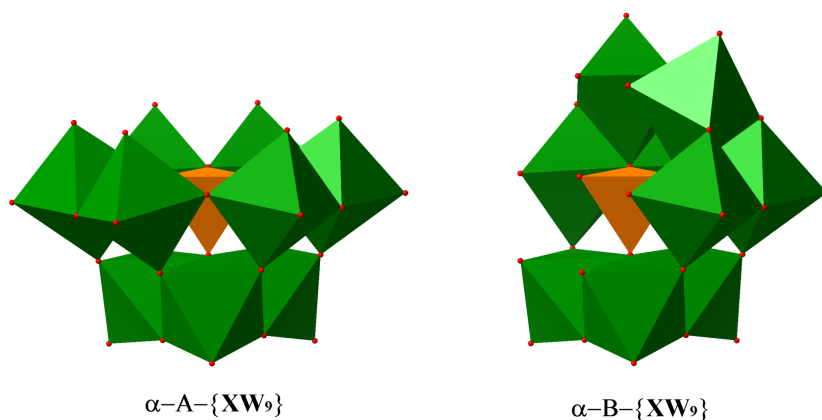


Figure 1.1: Polyhedral representation of the trilacunary derivatives of the α -*Keggin* anion: $\{\alpha\text{-A-XW}_9\}$ and $\{\alpha\text{-B-XW}_9\}$.

Trilacunary structures

Lacunary versions of the *Keggin* type anions result from the removal of one or more W centres. The trivacant species corresponds to the loss of a corner-shared group of $\{WO_6\}$ octahedra which leads to a A-type $\{XW_9\}$ unit or an edge-shared group of $\{WO_6\}$ octahedra leading to a B-type $\{XW_9\}$ unit (Figure 1.1). Note that B-type structures are commonly observed if the central atom has an unshared pair of electrons (e.g., As^{III} , Sb^{III}) [10]. A well known compound which can be described as a derivative of the B-type $\{XW_9\}$ unit is the tetramer $Na_{28}[\{(\alpha\text{-B-}As^{III}W_9O_{33})_4(WO_2)_4\}]$ (or $\{As_4W_{40}O_{140}\}$), in which four $\{AsW_9\}$ units are linked by additional $\{WO_2\}^{2+}$ groups [15].

1.2.2 Polyoxomolybdates

Polyoxomolybdate species - many of these are mixed-valence types - show an extreme variety of complicated structures and therefore great significance is attached to structural details. In this sense we will describe the spherical shaped $\{Mo_{132}\}$

type cluster [16, 17], the $\{Mo_{154}\}/\{Mo_{176}\}$ wheel shaped cluster [6, 7, 18] and even the largest inorganic cluster anion with 368 molybdenum atoms with lemon form [19, 20].

Giant Spherical Clusters: Inorganic Superfullerenes

In the case of polyoxomolybdates the pentagonal groups/motifs $\{(Mo)Mo_5\} \equiv \{(Mo)^0(Mo_5)^I\}$ consist of a central bipyramidal MoO_7 unit ($(Mo)^0$) sharing edges with 5 MoO_6 octahedra ($(Mo_5)^I$). These virtually planar groups are the basic units for quite a number of spherical-type clusters. When linkers are present in the reaction medium, for instance those of the classical $\{Mo_2^V O_4\}^{2+}$ type [21] which are typically built with a high formation tendency in reduced molybdate solutions in the presence of bidentate ligands, an icosahedral molecular system of 12 $\{(Mo)Mo_5\}$ pentagons and 30 linkers is built (Figure 1.2). Based on a topological concept, the cluster can be formulated as $\{Mo_{11}\}_{12} \equiv \{(Mo)^0(Mo_5)^I(Mo_2^V)^{II}\}_{12}$ (Figure 1.3), neglecting that the Mo atoms of each rather stable $\{Mo_2^V\}$ dumbbell belong to two adjacent $\{Mo_{11}\}$ groups. Interestingly, the $\{Mo_2^V\}$ groups themselves form a solid comparable to the C_{60} fullerene. The $\{Mo_{11}\}_{12}$ -type cluster corresponds to a fragment of Kepler's speculative model of the cosmos, as described in his early opus *Mysterium Cosmographicum* [22].

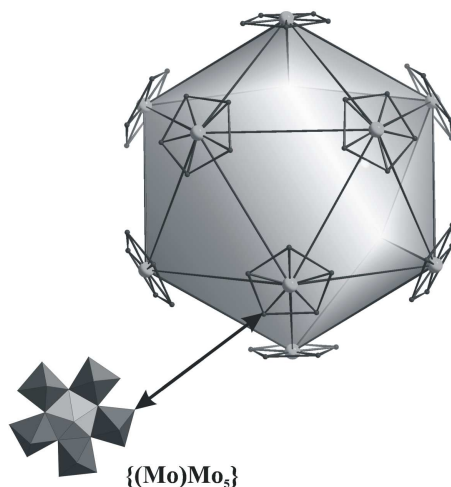


Figure 1.2: *Construction principle for clusters with icosahedral symmetry. The $\{(Mo)Mo_5\}$ units (polyhedral model with central pentagonal bipyramid in light grey) are the basis for the formation of the $\{(pent)_{12}(link)_{30}\}$ type clusters, where the $\{(Mo)Mo_5\}$ units define the vertices of an icosahedron. Adapted from reference [6].*

The ring shaped molecular big-wheels

The mentioned Keplerates are results of the "spherical disposition" of pentagonal $\{Mo_{11}\}$ building blocks with a C_5 symmetry whereas a "circular disposition" of the

deformed $\{Mo_{11}\}$ unit leads to the formation of $\{Mo_{154}\}$ and $\{Mo_{176}\}$ type clusters, commonly known as the big-wheel and giant-wheel type species, respectively [6]. Here the $\{Mo_{11}\}$ group differs from those present in the above-mentioned $\{Mo_{11}\}_{12}$ -type superfullerene in the sense that one of the peripheral MoO_6 octahedra is positioned in the way that the $\{Mo_{11}\}$ group shows only C_s symmetry. The structure of the ring-type species can therefore formally be represented as $[\{Mo_8\}\{Mo_2\}\{Mo_1\}]_m$, where $m = 14, 16$ for $\{Mo_{154}\}$ (Figure 1.3) and $\{Mo_{176}\}$, respectively. The $\{Mo_{154}\}$ cluster has an external diameter of 3.4 nm while that of $\{Mo_{176}\}$ is 4.1 nm [23].

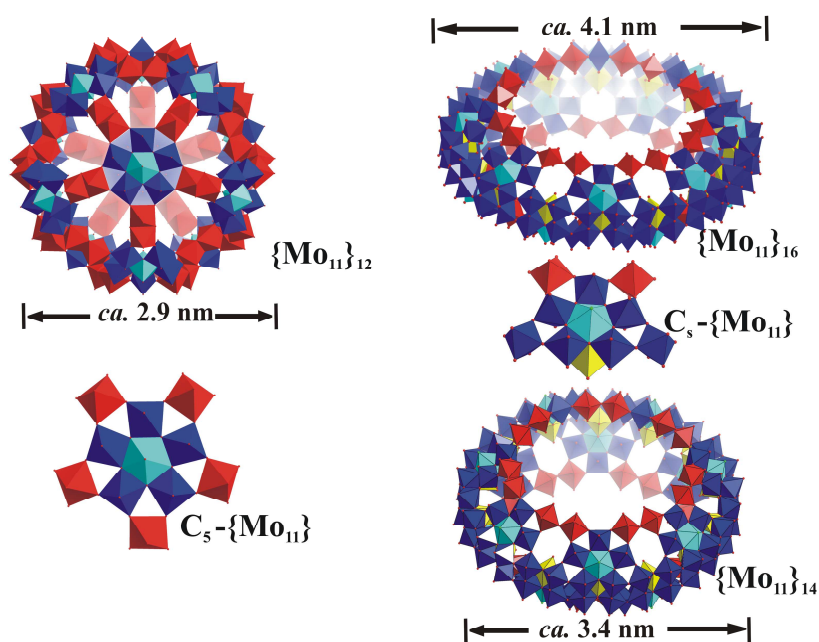


Figure 1.3: Molybdenum "brown" and "blue": Left: The spherical molybdenum "brown" type $\{Mo_{132}\}$ cluster is shown highlighting the constituent pentagonal $\{(Mo)Mo_5\}$ units (in cyan and blue) and $\{Mo_2\}$ units in red. Right: The wheel shaped molybdenum "blue" type $\{Mo_{154}\}$ and $\{Mo_{176}\}$ clusters are shown with the abundance of pentagonal $\{(Mo)Mo_5\}$ units (in blue and cyan) (Both types of $\{Mo_2\}$ units in red, $\{Mo_1\}$ units in yellow). Note the two different types of $\{Mo_{11}\}$ units highlighted. Adapted from reference [24].

The "Blue Lemon"

The special building units abundant in a potential "dynamic library" can form, via a type of "split and/or link process" (for instance the mentioned $\{(Mo)Mo_5\}$ units from larger ones which subsequently become linked) a class of molecular architectures upon slight variation of the boundary conditions. The $\{Mo_{368}\}$ cluster [19, 20] is such a molecular type (Figure 1.4); comparable to the size of hemoglobin (external diameter ca. 6 nm), this species is formed by the linking of 64 $\{Mo_1\}$, 32 $\{Mo_2\}$, and 40 $\{(Mo)Mo_5\}$ type units (32 with sulfate ligands and 8 without) via a remarkable

symmetry breaking process nicely noticeable on its surface.

The structure of the cluster anion can be considered as a hybrid between the $\{Mo_{176}\}/\{Mo_{154}\}$ type giant molecular wheels and the $\{Mo_{102}\}/\{Mo_{132}\}$ type clusters. The hybrid character manifests itself in the occurrence of 24 C_5 type $\{Mo_{11}\}$ units of the $\{Mo_{132}\}$ type ball shaped clusters together with 16 C_s type $\{Mo_{10}\}$ fragments of the related wheel shaped clusters having only one $\{MoO_6\}$ octahedron less. Although the C_5 $\{Mo_{11}\}$ groups are exactly identical to those of the spherical $\{Mo_{132}\}$ type Keplerate [7], the $\{Mo_{10}\}$ units are only identical to a fragment of the wheel type cluster C_s $\{Mo_{11}\}$ unit, i.e. the fragment without the 11th octahedron which is displaced. The blue lemon type cluster anion shows a combination of the central ball shaped fragment with D_{8d} symmetry $\{Mo_{288}\} \equiv \{Mo_{288}O_{784}(H_2O)_{192}(SO_4)_{32}\}$ and two capping fragments $\{Mo_{40}\} \equiv \{Mo_{40}O_{124}(H_2O)_{24}(SO_4)_8\}$ with C_{4v} symmetry.

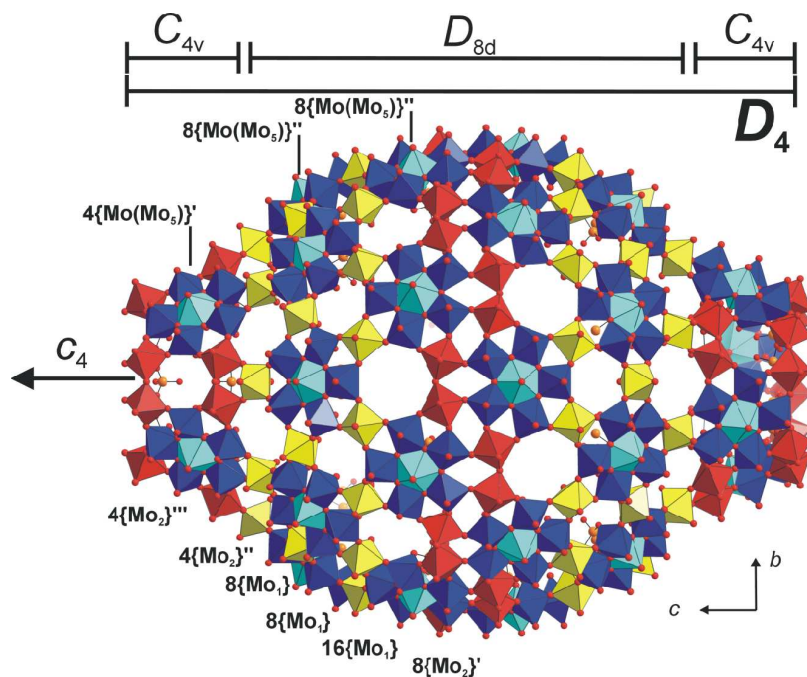


Figure 1.4: $[H_x Mo_{368} O_{1032} (H_2O)_{240} (SO_4)_{48}]^{48-}$ cluster anion in polyhedral representation showing the different building blocks and large areas of different local symmetry; building units $\{Mo_1\}$ (yellow), $\{Mo_2\}$ (red), $\{(Mo)Mo_5\}$ (blue with blue-turquoise pentagonal bipyramids). Adapted from reference [19].

1.3 Goals of the project: defining the problem

The challenging aspects provided by this research were :

- The "activation" of the cavity of the $\{As_4M_{40}O_{140}\}$ -type cryptand leading to the options to encapsulate cationic as well as anionic "guests".
- The exploitation of the host potential in the spherical polyoxomolybdates.
- The possibility to study the of guest "uptake and release" in case of the spherical capsules in solution.

Bibliography

- [1] (a) J. M. Lehn, *"Supramolecular Chemistry, Concepts and Perspectives"*, VCH, Weinheim, **1995**; (b) J. M. Lehn, *Pure Appl. Chem.* **1978**, *50*, 871.
- [2] J. M. Lehn, *Angew. Chem., Int. Ed. Engl.* **1988**, *27*, 89.
- [3] J. M. Lehn, *Angew. Chem., Int. Ed. Engl.* **1990**, *29*, 1304.
- [4] *"Supramolecular Chemistry"*, (Eds.: V. Balzani and I. DeCola), Kluwer, Dordrecht, **1992**.
- [5] P. N. W. Baxter, *"Comprehensive Supramolecular Chemistry" Vol. 9*, (Eds.: J. L. Atwood, J. E. D. Davies, D. D. MacNicol, F. Vögtl and J.-M. Lehn), Pergamon/Elsevier, Oxford, **1996**, pp. 165.
- [6] A. Müller and S. Roy, *Coord. Chem. Rev.* **2003**, *245*, 153.
- [7] A. Müller P. Kögerler, H. Bögge, *Structure and Bonding* **2000**, *96*, 203.
- [8] (a) D.G. Kurth, P. Lehmann, D. Volkmer, H. Cölfen, M.J. Koop, A. Müller, A. Du Chesne, *Chem. Eur. J.* **2000**, *6*, 385; (b) D.G. Kurth, D. Volkmer, M. Ruttorf, B. Richter, A. Müller, *Chem. Mater.* **2000**, *12*, 2829; (c) D.G. Kurth, P. Lehmann, D. Volkmer, A. Müller, D. Schwahn, *J. Chem. Soc., Dalton Trans.* **2000**, 3989; (d) F. Caruso, D.G. Kurth, D. Volkmer, M.J. Koop, A. Müller, *Langmuir* **1998**, *14*, 3462; (e) D. Volkmer, A. Du Chesne, D.G. Kurth, H. Schnablegger, P. Lehmann, M.J. Koop, A. Müller, *J. Am. Chem. Soc.* **2000**, *122*, 1995; (f) S. Polarz, B. Smarsly, C. Göltner, M. Antonietti, *Adv. Mater.* **2000**, *12*, 1503; (g) S. Polarz, B. Smarsly, M. Antonietti, *ChemPhysChem.* **2001**, *2*, 457; (h) L. An, J.M. Owens, L.E. McNeil, J. Liu, *J. Am. Chem. Soc.* **2002**, *124*, 13688; (i) D. Gatteschi, L. Pardi, A.L. Barra, A. Müller, J. Döring, *Nature* **1991**, *354*, 463.
- [9] (a) A. Müller, E. Diemann, C. Kuhlmann, W. Eimer, C. Serain, T. Tak, A. Knöchel, P.K. Pranzas, *Chem. Commun.* **2001**, 1928; (b) T. Liu, *J. Am. Chem. Soc.* **2002**, *124*, 10942; *ibid* **2003**, *125*, 312; (c) See also: T. Liu, E. Diemann, H. Li, A. Dress, A. Müller, *Nature* **2003**, *426*, 59.
- [10] A. Müller, F. Peters, M. T. Pope and D. Gatteschi, *Chem. Rev.*, **1998**, *98*, 239.

- [11] M.T. Pope and A. Müller, *Angew. Chem., Int. Ed. Engl.* **1991**, *30*, 34.
- [12] L. C. W. Baker, V. S. Baker, K. Eriks, M. T. Pope, M. Shibata, O. W. Rollins, J. H. Fang, L. K. Koh, *J. Am. Chem. Soc.* **1966**, *88*, 2329
- [13] L. C. W. Baker, J. S. Figgis, *J. Am. Chem. Soc.* **1970**, *92*, 3794.
- [14] M. T. Pope, *Heteropoly and Isopoly Oxometalates*, Springer, Berlin, **1983**.
- [15] M. Leyrie, G. Herv, *Nouv. J. Chim.* **1978**, *2*, 233.
- [16] A. Müller, P. Kögerler, C. Kuhlmann, *Chem. Commun.* **1999**, 1347.
- [17] A. Müller, E. Krickemeyer, H. Bögge, M. Schmidtman, F. Peters, *Angew. Chem. Int. Ed.* **1998**, *37*, 3360.
- [18] A. Müller, C. Serain, *Acc. Chem. Res.* **2000**, *33*, 2.
- [19] A. Müller, E. Beckmann, H. Bögge, M. Schmidtman, A. Dress, *Angew. Chem. Int. Ed.* **2002**, *41*, 1162.
- [20] A. Müller, B. Botar, S. K. Das, H. Bögge, M. Schmidtman, A. Merca, *Polyhedron* **2004**, *23*, 2381.
- [21] H.K. Chae, W.G. Klemperer, T.A. Marquart, *Coord. Chem. Rev.* **1993**, *128*, 209.
- [22] (a) J. Kepler, *Mysterium Cosmographicum* **1956**; see also (b) M. Kemp, *Nature* **1998**, *393*, 123.
- [23] A. Müller, M. Koop, H. Bögge, M. Schmidtman, C. Beugholt, *Chem. Commun.* **1998**, 1501.
- [24] S. Roy, Ph. D. Thesis, Giant polyoxomolybdates: Syntheses, structure and stability studies; From syntheses of extended structures to novel host design, stability investigations in solution and perspectives for a future mechanistic study, University of Bielefeld, **2005**.

Chapter 2

Publications

- 2.1** *A Small Cavity with Reactive Internal Shell Atoms Spanned by Four $\{As(W/V)_9\}$ -Type Building Blocks Allows Host Guest Chemistry under Confined Conditions*
 A. Müller, M. T. Pope, *A. Merca*, H. Bögge, M. Schmidt-
 mann, J. van Slageren, M. Dressel, D. G. Kurth
Chem. Eur. J. 2005, accepted.

Contribution of A. Merca to the following publication:

- Synthesis and characterization (electronic absorption as well as vibrational spectra, redox titrations, elemental analysis) of the new compounds.

- 2.2** *Trapping Cations in Specific Positions in Tuneable "Artificial Cell" Channels: New Nanochemistry Perspectives*
 A. Müller, S. K. Das, S. Talismanov, S. Roy, E. Beck-
 mann, H. Bögge, M. Schmidtman, *A. Merca*, A. Berkle,
 L. Allouche, Y. Zhou, L. Zhang
Angew. Chem. Int. Ed. 2003, *42*, 5039-5044.

Contribution of A. Merca to the following publication:

- Synthesis and characterization (electronic absorption as well as vibrational spectra, redox titrations, elemental analysis) of the new compound **6** in the paper.
 $[NH_3^+CONH_2]_{28}Na_{11}([NH_3^+CONH_2]_{20}+Na_{13}) \subset \{(Mo^{VI})Mo_5^{VI}O_{21}(H_2O)_6\}_{12}$
 $\{Mo_2^V O_4(SO_4)\}_{30} \cdot ca.200 H_2O$

2.3 *Artificial Cell Decision about Metal Cations Entrance: the "Stable" Aqua Complexes Get Trapped Above the Pores others Slip Out its Water Coat and the Cations Enter*

A. Müller, A. Merca, H. Bögge, M. Schmidtman, A. Berkle

Chem. Commun. 2005, to be submitted.

Contribution of A. Merca to the following publication:

- Synthesis and characterization (electronic absorption as well as vibrational spectra, redox titrations, elemental analysis) of the new compound.

2.4 *Temperature-Dependent Reversible Li⁺ Uptake/Release Equilibrium at Metal-Oxide Nanocontainer-Pores*

A. Müller, D. Rehder, E.T.K. Haupt, A. Merca, H. Bögge, M. Schmidtman, G. Heinze-Brückner

Angew. Chem. Int. Ed. 2004, *43*, 4466-4470; Corrigendum: *43*, 5115.

Contribution of A. Merca to the following publication:

- Synthesis and characterization (electronic absorption as well as vibrational spectra, redox titrations, elemental analysis) of the new compound.

2.5 *On the Complex Hedgehog Shaped Cluster Species Containing 368 Mo Atoms: Simple Preparation Method, New Spectral Details and Information About the Unique Formation*

**A. Müller, B. Botar, S. K. Das, H. Bögge, M. Schmidt-
mann, A. Merca**

***Polyhedron* 2004, 23, 2381-2385.**

Contribution of A. Merca to the following publication:

- Characterization of the $\{Mo_{368}\}$ type cluster obtained by an improved synthesis (electronic absorption as well as vibrational spectra, redox titrations, elemental analysis) and investigations of the stability through variation of cations .

A Small Cavity with Reactive Internal Shell Atoms Spanned
by Four {As(W/V)₉}-Type Building Blocks Allows Host-Guest
Chemistry under Confined Conditions

Achim Müller,^{*[a]} Michael T. Pope,^{*[b]} Alice Merca,^[a] Hartmut
Bögge,^[a] Marc Schmidtman,^[a] Joris van Slageren,^[c] Martin
Dressel,^[c] and Dirk G. Kurth^[d]

[a] Prof. Dr. A. Müller, Dipl.-Chem. A. Merca, Dr. H.
Bögge, M. Schmidtman
Lehrstuhl für Anorganische Chemie I
Fakultät für Chemie der Universität
Postfach 100131, 33501 Bielefeld (Germany)
Fax: (+49) 521-106-6003
E-mail: a.mueller@uni-bielefeld.de

[b] Prof. Dr. M. T. Pope
Department of Chemistry, Georgetown University
Washington, DC 20057-1227 (USA)
Fax: (+1)202-687-6209
E-mail: popem@georgetown.edu

[c] Dr. J. van Slageren, Prof. Dr. M. Dressel
Physikalisches Institut, Universität Stuttgart
Pfaffenwaldring 57, 70550 Stuttgart (Germany)

[d] Dr. D. G. Kurth
Max-Planck-Institute of Colloids and Interfaces
14424 Potsdam (Germany)

Abstract: The reaction of $[\text{H}_2\text{As}^{\text{III}}\text{W}_{18}\text{O}_{60}]^{7-}$ with VO^{2+} and SO_4^{2-} ions in aqueous solution leads to a $\text{V}^{\text{IV}}/\text{V}^{\text{V}}$ mixed-valence cluster anion containing the $\{\text{As}_4\text{M}_{40}\text{O}_{140}\}$ -type cryptand which has a high formation tendency. An important result is that it exhibits a new type of reactive internal cavity shell. The correspondingly obtained compound $\text{Na}(\text{NH}_4)_{20}[\{(\text{V}^{\text{IV}}\text{O}(\text{H}_2\text{O}))(\text{V}^{\text{IV}}\text{O})_2(\text{SO}_4)_2\}\{(\text{As}^{\text{III}}\text{W}_9\text{O}_{33})_2(\text{As}^{\text{III}}\text{W}_{7.5}\text{V}_{1.5}\text{O}_{31})_2(\text{WO}_2)_4\}] \cdot 40 \text{H}_2\text{O}$ **1**, which can also be synthesized from an educt with the preorganized cryptand, was characterized by elemental and thermogravimetric analyses (determination of crystal water content), redox titrations (determination of the number of V^{IV} centres), electronic absorption as well as vibrational spectra, single crystal X-ray structure analysis (including bond valence sum calculations) and magnetic susceptibility measurements. The relatively small central cavity - formed by the linking of four $\{\text{AsM}_9\}$ -type lacunary units ($\text{M} = \text{W}/\text{V}$) by four WO_6 octahedra - allows positioning of a variety of cationic as well as anionic "guests" under confined conditions according to a new approach: replacement of some of the W by V atoms leads to high reactivity of the internal cavity shell as a result of relatively weak VO bonds compared to the WO situation. This allows an interesting "encapsulation chemistry" with new options. In the present case the cavity contains besides an arrangement of three V^{IV} centres, two sulphate groups replacing O atoms of the $\{\text{AsM}_9\}$ units as well as an interesting hydrogen bond situation.

Keywords: polyoxometalate · magnetism · cryptand · encapsulation chemistry

Introduction

Polyoxometalates constitute - due to their structural variety as well as their relevance to several fields ^[1-4] - a unique class of inorganic species. Whereas in recent years, a variety of very large polyoxomolybdates have been synthesized and structurally characterized, for example the wheel-shaped anions of the type Mo_{154} , Mo_{176} ^[5,6] as well as the corresponding derivative Mo_{248} ,^[7] the spherical icosahedral capsule Mo_{132} ,^[8] and the "hedgehog-shaped" Mo_{368} -type cluster species,^[9] the chemistry of polyoxotungstates is not so rich regarding nanosized complexes (for reasons see reference [9a]; but note the existence of the W_{148} anion^[10]). On the other hand, polyoxotungstates offer other options: special polyoxotungstate (VI) matrices for instance are ideal for embedding "guests", e.g. in the form of magnetic centres. In this sense trilacunary-type XW_9 units used as building blocks are of special importance. When three corner-shared octahedra are removed from a Keggin ion, the so-called A-type trilacunary anion is obtained while the loss of three edge-shared octahedra results in a B-type trilacunary anion. The latter type, which is obtained if the central atom such as As^{III} has a lone pair of electrons, can be used, e.g. as building block for the synthesis of sandwich-like mixed- and non-

mixed-valence complexes of the type $[(VO)_3(XW_9O_{33})_2]^{n-}$ ($n= 11, 12$; $X= As^{III}, Sb^{III}$) in which two α -B- $[XW_9O_{33}]^{9-}$ ($X= As^{III}, Sb^{III}$) units are linked by a belt of three VO^{2+} cations ^[11,12] (see also reference [13]). Quite a variety of encapsulation-type investigations were performed based on the (related) cryptand $\{As_4W_{40}O_{140}\}$, in which four B-type trilacunary units are linked together by four WO_6 octahedra, e.g. in clusters with the general formula $[M_1M_2Z_m(H_2O)_2As_4W_{40}O_{140}]^{x-}$, where M_1 and M_2 ($m=0$ or 1) are alkali and/or alkaline earth cations and Z , first-row transition metal cations (like Co^{2+}).^[14-16] Here we demonstrate the option for a new type of encapsulation chemistry via an unprecedented activation of the $\{As_4W_{40}O_{140}\}$ internal shell cryptand atoms, which is based on the substitution of tungsten atoms of the XW_9 units by vanadium centres with the consequence of an activation of the oxygen atoms at the internal cavity shell. In this context we report here the compound $Na(NH_4)_{20}[\{(V^{IV}O(H_2O))(V^{IV}O)_2(SO_4)_2\}\{(As^{III}W_9O_{33})_2(As^{III}W_{7.5}V_{1.5}O_{31})_2(WO_2)_4\}] \cdot 40 H_2O$ **1** \equiv $Na(NH_4)_{20}$ **1a** $\cdot 40 H_2O$, containing three V^{IV} centres and two sulphates in the small anion central cavity which could be made possible due to the replacement of W^{VI} by V^V atoms leading to increased reactivity of the O (-V)atoms. The present investigation demonstrates the

general option to place a variety of magnetic centres adjacent to *anionic guests* like sulphate ions under confined conditions in a cryptand, as well as the option to generate interesting hydrogen bonding situations where water ligands coordinated to the metal centres are involved. Important in this context is the small cavity space which can lead, in principle, to strong exchange interactions.

Results and Discussion

Compound **1** was primarily prepared by heating an aqueous solution of the sodium salt of $[\text{H}_2\text{As}^{\text{III}}\text{W}_{18}\text{O}_{60}]^{7-}$ **2a**^[17] and $\text{VOSO}_4 \cdot 5\text{H}_2\text{O}$ and was characterized by elemental and thermogravimetric analyses (for determination of crystal water content), electronic absorption as well as vibrational spectra, single crystal X-ray structure analysis (including bond valence sum calculations), magnetic susceptibility measurements and redox titrations (for the determination of the number of V^{IV} centres). The mentioned reaction occurs due to the high formation tendency of the anionic $\{\text{As}_4\text{M}_{40}\text{O}_{140}\}$ type cryptand. (**1** can correspondingly also be obtained from the preorganized cryptand abundant in the compound $\text{Na}_{27}[\text{Na}\{(\text{As}^{\text{III}}\text{W}_9\text{O}_{33})_4(\text{WO}_2)_4\}] \cdot 60 \text{H}_2\text{O}$ **3**^[14] (see Experimental Section), but unfortunately

the crystal quality is not as good.) Although the basic framework, i.e. the cryptand skeleton of **1a**, is formally similar to that of the anions **4a** of $(\text{NH}_4)_{21}[\{(\text{NH}_4)_3(\text{Co}^{\text{II}}\text{H}_2\text{O})_2\}\{(\text{As}^{\text{III}}\text{W}_9\text{O}_{33})_4(\text{WO}_2)_4\}] \cdot 19 \text{ H}_2\text{O}$ **4** \equiv $(\text{NH}_4)_{21}$ **4a** \cdot $19 \text{ H}_2\text{O}$ ^[15,18] and **5a** of $\text{Na}_{23}[\{\text{Na}(\text{Na}_4)\}\{(\text{As}^{\text{III}}\text{W}_9\text{O}_{33})_4(\text{WO}_2)_4\}] \cdot 2 \text{ Cl} \cdot n \text{ H}_2\text{O}$ **5** \equiv Na_{23} **5a** \cdot $n \text{ H}_2\text{O}$ (reformulated here), ^[19] it contains a new type of cavity reactivity and related interesting "encapsulations" (details below).

Each cluster anion of **1a** is "linked" in the crystal lattice to two neighbouring anions by disordered $\text{Na}(\text{H}_2\text{O})_3$ units forming infinite parallel chains (Figure 1a). A characteristic feature of these parallel chains is that they are rotated relative to neighbouring chains by 180° parallel to the c axis, translated by $c/2$, and are then connected through additional "Na-O bonds" thus forming a layer structure. Interestingly, exactly the same number of Na^+ cations was obtained (one Na^+ cation/formula unit) in spite of varying the NH_4^+ concentration in the reaction medium. This reemphasizes the possible importance of the presence of appropriate countercations for the assembly of (large) polyoxometalate structures.

The cluster anion **1a** (Figure 1b) is as mentioned above built up by four trilacunary $\alpha\text{-B-As(W/V)}_9$ units connected by

four WO_6 octahedra, thereby generating a cyclic arrangement with a small central cavity. Two of the opposite AsM_9 units have two tungsten atoms (mostly) replaced by V^{V} centres corresponding to a related disorder of the anions in the crystal lattice, while the occupancy factor is ca. 25% for W and 75% for V atoms. Each trilacunary unit has six oxygen atoms available for coordination; in Figure 1b the corresponding 4×6 oxygen atoms (red) are marked by a black rectangle. Four of these oxygen atoms are shared with neighbouring connecting WO_6 octahedra (see above), i.e. two lacunary units share one WO_6 octahedron. The remaining two oxygen atoms participate in two coordination modes: (1) each of the two lacunary units containing only W atoms (these are shown on the left and right in Figure 1b) is linked to an $\text{O}=\text{V}^{\text{IV}}\text{O}_4$ square pyramid by sharing corners, i.e. at the positions marked as S2 in Figure 1c where Co^{2+} is found in **4a**; (2) each of the two lacunary units containing V centres (top and bottom in Figure 1b) is linked to a sulphate group by sharing corners, i.e. at the positions marked as S2' in Figure 1c where NH_4^+ ions are found in **4a**. Referring to the four bridging WO_6 groups: each of these shares one corner with one of the $\text{O}=\text{V}^{\text{IV}}\text{O}_4$ square pyramids and another corner with a central $\text{V}^{\text{IV}}\text{O}_5(\text{H}_2\text{O})$ octahedron, defining the S1 site, which is occupied in **4a** by an NH_4^+

ion. Interestingly, the sulphate groups are stabilized by short hydrogen bonds between the O atoms of the sulphate group and the H₂O ligand of the central V^{IV}O₅(H₂O) octahedron (Figure 2a).

Due to its small central cavity and the reactive internal cavity shell, the present {As₄M₄₀O₁₄₀}-type cryptand (see also references [14,15]) is a remarkable "host" for the incorporation of guest cations and anions, and especially of magnetic centres in presence of anions under confined conditions. The option of making the lacunary fragments more reactive leads to sulphate ligation which is caused by the partial replacement of W by V atoms, and consequently to weakened metal-oxygen bonds. Under changed reaction conditions via a synthesis similar to that of compound **1**^[20] but with a lower pH value, the compound (NH₄)₂₀[{(V^{IV}O(H₂O)(V^{IV}O)₂)(NH₄)₂}{(As^{III}W₉O₃₃)₄(WO₂)₄}] · 40 H₂O **6** ≡ (NH₄)₂₀ **6a** · 40 H₂O,^[20] can be obtained. This is similar to **1** but with the difference that the W atoms are not substituted by V atoms at all and the positions of the sulphate ligands are correspondingly (formally) occupied by NH₄⁺ cations. This observation corresponds to the known fact that substitution reactions of the type discussed here, involving a weakening the WO bonds, are favoured at higher pH values (see e.g. reference [3]). The complete results of

the single crystal structure analysis of **6a** which are not of interest in the present context are not reported here, only the characterization by unit cell dimensions, analytical data and characteristic magnetic data which show clearly the three encapsulated V^{IV} centres (see below).

Spectroscopic and Magnetic Properties

The electronic absorption spectrum (Vis/NIR region) of **1** in aqueous solutions shows bands at ≈ 690 (sh) and ≈ 860 nm which arise from d-d (V^{IV}) and/or V^{IV}→W^{VI} (IVCT) charge transfer transitions^[21] confirming the presence of the V^{IV} centres.

The magnetic susceptibility of the present compound **1** was measured as a function of temperature. These data are shown in Figure 3 as the product of molar magnetic susceptibility and temperature against temperature. The χT value at high temperature is 1.08 emuK⁻¹mol⁻¹ which is close to the expected spin only value for three $S = \frac{1}{2}$ ions ($\chi T = 1.08$ emuKmol⁻¹; the average g value of vanadyl ions was taken to be 1.96^[22]). On lowering the temperature the χT product decreases first slightly, then more rapidly. At the lowest temperatures, it seems to be approaching a limiting value. Fitting χ^{-1} versus T to the Curie-Weiss law ($35 \text{ K} \leq T \leq 300 \text{ K}$), yields a Curie constant of 1.12 emuKmol⁻¹, close

to the room temperature χT value, and a Weiss temperature of $\theta = -13.2$ K, indicative of predominantly antiferromagnetic exchange interactions. The χT versus T data can also be fitted to the van Vleck formula for the susceptibility,^[23] assuming nearest neighbour exchange interactions only. Although the three vanadyl ions form a triangle in the structure (Figure 2b), there is interestingly no superexchange pathway between vanadyl ions 1 and 3, but only between neighbored vanadyl ions 1 and 2 and 2 and 3. This means that magnetically, the system can be considered formally as a linear trimer. The superexchange pathway is $V^{IV}-O-W-O-V^{IV}$ and the spin Hamiltonian was defined as $\mathbf{H} = J (\mathbf{S}_1 \cdot \mathbf{S}_2 + \mathbf{S}_2 \cdot \mathbf{S}_3)$. The least-squares fit leads to an exchange interaction constant of $J = 13.2 \pm 0.5 \text{ cm}^{-1}$ and $g = 1.94$. As mentioned above there is no direct superexchange pathway between the outer vanadyl ions and indeed, including a next-nearest neighbour interaction between the two outer vanadyl ions does not improve the fit significantly.

The compound $(\text{NH}_4)_{23} [\{ (\text{K} (\text{V}^{IV}\text{O})_2) \} \{ (\text{As}^{\text{III}}\text{W}_9\text{O}_{33})_4 (\text{WO}_2)_4 \}] \cdot n \text{H}_2\text{O}$, the anion of which corresponds to **1a** without the central V^{IV} atom, has been earlier examined by magnetic susceptibility measurements and ESR spectroscopy.^[24] The susceptibility data between 5 and 300 K show no magnetic

coupling between the vanadium ions, in agreement with the above given results for **1**. However, based upon single crystal ESR spectra a very weak antiferromagnetic exchange interaction with $J = -0.073 \text{ cm}^{-1}$ could be reliably determined and represents a superexchange pathway through a sequence of even ten W-O bonds.

Compound **6**, in which no substitution of W atoms by V^V has occurred was also studied by magnetic susceptibility measurements. The room temperature χT value of $1.02 \text{ emuKmol}^{-1}$ is consistent with the presence of three $S = \frac{1}{2}$ ions. The χT product decreases with decreasing temperature, and reaches a small plateau at 5 K ($\chi T \approx 0.4 \text{ emuKmol}^{-1}$) before decreasing further. The magnetic susceptibility curve was fitted assuming a linear trinuclear cluster without exchange interactions between the outer ions, as for compound **1** (Figure 4). The obtained exchange interaction is $J = 10.7 \pm 0.5 \text{ cm}^{-1}$, with $g = 1.92$, is slightly smaller than that of **1** while the difference should be due to the presence of the sulphates in **1a**.

Conclusions and Perspectives

The present discovery shows, in principle, the options of incorporating a variety of (cationic) magnetic centres (see also references [19, 25-27]) together with anions in the

small cavity of the cryptand. On the other hand, there is the option to investigate interesting related hydrogen bonds situations between oxo anions and H₂O ligands of the metal centres under confined conditions.

The cavity discussed here is much smaller than in some larger polyoxomolybdates which were mentioned in the introduction, e.g. in the case of our spherical porous capsules of the type $\{(Mo)Mo_5\}_{12}\{Linkers\}_{30}$ ^[28] which can also encapsulate (cationic) magnetic centres ("A *single-molecule anion made of 132 molybdenum atoms forms a spherical oxide cage that can bind several cations*" was mentioned in a recent highlight referring to that^[18] in which the present $\{As_4W_{40}\}$ type cryptand^[29] was discussed in that context too). A further option for the future is to study cation-inside-outside-exchanges by NMR as was done in an interesting earlier study for the present type of cryptand system (see reference [2c]) and which now could be extended to situations in presence of "encapsulated" anions. Additionally, there is - according to preliminary experiments - the possibility to generate interesting magnetic micelles with cationic surfactants from the cluster anions reported here.^[30]

Experimental Section

Preparation of 1 (Method 1): The sodium salt of **2a** was prepared according to reference [17]. To an aqueous solution of CH₃COONa/CH₃COOH buffer (pH=4.0) - (60 mL) and VOSO₄ · 5H₂O (2 g, 8 mmol), the sodium salt of **2a** (3 g) was added. The resulting brown mixture was stirred for 48 h at room temperature, and then heated to 70-80 °C. After addition of NH₄Cl (5 g, 93.4 mmol) the solution was kept at this temperature for 30 min and then filtered while still hot. After 6 days dark brown crystals of **1** were filtered. Yield: 1.73 g, (54% based on W).

IR (solid, KBr pellet): $\nu = 1616$ (m) [δ (H₂O)], 1402 (s) [δ_{as} (NH₄)], 1209 (w), 1126 (w), 1022 (sh) [all ν_{as} (SO₄)], 956 (s) [ν (W=O) / ν (V=O)], 877 (m), 833 (m), 704 (sh), 621 (m) cm⁻¹ [ν_{as} (W-O-W) / ν_{as} (W-O-V)]; Raman (solid, KBr dilution, $\lambda_e=1064$ nm): $\nu \approx 886$ (m), 969 (w) cm⁻¹ [ν (W=O) / ν (V=O)]; UV/VIS (in H₂O): λ_{max} (ϵ) = 862 (208), 694 nm (232 mol⁻¹ dm³ cm⁻¹); elemental analysis calcd (%) for H₁₆₂As₄N₂₀NaO₁₈₈S₂V₆W₃₇ (10946.38): N 2.47, Na 0.2, S 0.55, V 2.8, V(IV) 1.5; found: N 2.6, Na 0.2, S 0.3, V 3, V(IV) 1.3.

Method 2. To an aqueous solution of CH₃COONa/CH₃COOH buffer (pH=4.0) (60 mL) and VOSO₄ · 5H₂O (2 g, 8 mmol),

$\text{Na}_{27}[\text{Na}\{(\text{As}^{\text{III}}\text{W}_9\text{O}_{33})_4(\text{WO}_2)_4\}] \cdot 60 \text{ H}_2\text{O}$ **3** (3 g, 0.26 mmol) was added. **3** was prepared according to reference [14]). The resulting brown mixture was stirred for 48 h at room temperature, and then heated to 70–80 °C. After addition of NH_4Cl (5 g, 93.4 mmol) the solution was kept at this temperature for 30 min and then filtered while still hot. After 5 days the dark brown precipitated crystals of **1** were filtered. Yield: 0.5 g, (18% based on W).

As the quality of the crystals obtained by the alternative preparation method was not as good as those of method 1 the obtained structural data were not given here, though they confirmed the reported structure. Also the analytical, spectroscopic and magnetic data are identical.

Single Crystal X-ray Structure Determination: Crystals suitable for X-ray crystal structure determination were obtained with the above given synthetic method with the difference that only 1.5 g NH_4Cl was used. This led to better and bigger crystals but also to a longer crystallization time (6 weeks). The X-ray crystal structure determination presented here was performed on the crystals obtained primarily.

Crystal data for **1**: $\text{H}_{162}\text{As}_4\text{N}_{20}\text{NaO}_{188}\text{S}_2\text{V}_6\text{W}_{37}$, $M = 10946.38 \text{ g mol}^{-1}$, orthorhombic, space group Pnma , $a = 26.201(2)$, $b = 28.257(2)$, $c = 23.1844(14) \text{ \AA}$, $V = 17165(2) \text{ \AA}^3$, $Z = 4$, ρ

= 4.236 g/cm³, μ = 25.914 mm⁻¹, $F(000)$ = 19428, crystal size = 0.30 x 0.25 x 0.15 mm. Crystals of **1** were removed from the mother liquor and immediately cooled to 183(2) K on a Bruker AXS SMART diffractometer (three circle goniometer with 1K CCD detector, Mo-K α radiation, graphite monochromator; hemisphere data collection in ω at 0.3° scan width in three runs with 606, 435 and 230 frames (θ = 0, 88 and 180 °) at a detector distance of 5 cm). A total of 98713 reflections ($1.17 < \theta < 27.02^\circ$) were collected of which 19072 reflections were unique ($R(\text{int}) = 0.0644$). An empirical absorption correction using equivalent reflections was performed with the program SADABS. The structure was solved with the program SHELXS-97 and refined using SHELXL-93 to $R = 0.0447$ for 14594 reflections with $I > 2 \sigma(I)$, $R = 0.0666$ for all reflections; max/min residual electron density 3.798 and -3.066 eÅ⁻³. (SHELXS/L, SADABS from G.M. Sheldrick, University of Göttingen 1993/97; structure graphics with DIAMOND 2.1 from K. Brandenburg, Crystal Impact GbR, 2001.) Further details of the crystal structure investigation(s) (excluding structure factors) for **1** may be obtained from the Fachinformationszentrum Karlsruhe, 76344 Eggenstein-Leopoldshafen, Germany (fax: (+49) 7247-808-666; e-mail: crysdatab@fiz-karlsruhe.de) on quoting the depository number CSD-414216.

Magnetic Measurements: Magnetic susceptibility measurements were performed on a powder sample using a Quantum Design MPMS XL7 SQUID magnetometer. The data were corrected for the diamagnetic contributions to the molar magnetic susceptibility using Pascal's constants and also for temperature independent paramagnetism.

Acknowledgements

We thank the Fonds der Chemischen Industrie, the Deutsche Forschungsgemeinschaft, the Volkswagen Stiftung and the European Union (Brussels) for financial support. A. Merca

thanks the "Graduiertenkolleg Strukturbildungsprozesse", Universität Bielefeld, for a fellowship. The authors thank Dipl.-Chem. Alois Berkle for some analyses and Dr. Paul Kögerler for his collaboration.

References

- [1] M. T. Pope, *Heteropoly and Isopoly Oxometalates*, Springer, Berlin, **1983**.
- [2] a) *Polyoxometalate Chemistry: From Topology via Self-Assembly to Applications* (Eds.: M. T. Pope, A. Müller), Kluwer, Dordrecht, **2001**; b) *Polyoxometalate Molecular Science* (Eds.: J. J. Borrás-Almenar, E. Coronado, A. Müller, M. T. Pope), Kluwer, Dordrecht, **2003**; c) *Polyoxometalates: From Platonic Solids to Anti-Retroviral Activity* (Eds.: M. T. Pope, A. Müller), Kluwer, Dordrecht, **1994** (with special reference to the article of R. Thouvenot, M. Michelon, A. Tézé, G. Hervé, pp. 177-190); d) A. Müller, S. Roy in *The Chemistry of Nanomaterials: Synthesis, Properties and Applications* (Eds.: C. N. R. Rao, A. Müller, A. K. Cheetham), Wiley-VCH, Weinheim, **2004**, pp. 452-475.
- [3] M. T. Pope, A. Müller, *Angew. Chem.* **1991**, *103*, 56-70; *Angew. Chem. Int. Ed.* **1991**, *30*, 34-48.

- [4] A. Müller, F. Peters, M. T. Pope, D. Gatteschi, *Chem. Rev.* **1998**, *98*, 239-271.
- [5] a) A. Müller, P. Kögerler, C. Kuhlmann, *Chem. Commun.* **1999**, 1347-1358; b) A. Müller, C. Serain, *Acc. Chem. Res.* **2000**, *33*, 2-10.
- [6] A. Müller, S. Roy, *Coord. Chem. Rev.* **2003**, *245*, 153-166.
- [7] A. Müller, S. Q. N. Shah, H. Bögge, M. Schmidtman, *Nature* **1999**, *397*, 48-50.
- [8] A. Müller, E. Krickemeyer, H. Bögge, M. Schmidtman, F. Peters, *Angew. Chem.* **1998**, *110*, 3567-3571; *Angew. Chem. Int. Ed.* **1998**, *37*, 3360-3363.
- [9] a) A. Müller, E. Beckmann, H. Bögge, M. Schmidtman, A. Dress, *Angew. Chem.* **2002**, *114*, 1210-1215; *Angew. Chem. Int. Ed.* **2002**, *41*, 1162-1167; b) A. Müller, B. Botar, S. K. Das, H. Bögge, M. Schmidtman, A. Merca, *Polyhedron* **2004**, *23*, 2381-2385.
- [10] K. Wassermann, M. H. Dickman, M. T. Pope, *Angew. Chem.* **1997**, *109*, 1513-1516; *Angew. Chem. Int. Ed.* **1997**, *36*, 1445-1448.
- [11] P. Mialane, J. Marrot, E. Rivière, J. Nebout, G. Hervé, *Inorg. Chem.* **2001**, *40*, 44-48.
- [12] T. Yamase, B. Botar, E. Ishikawa, K. Fukaya, *Chem. Lett.* **2001**, 56-57.

- [13] B. Botar, H. Bögge, A. Müller, *Bull. Pol. Acad. Sc. Chem.* **2002**, *50*, 139-144 (Dedicated to Prof. A. Bielanski).
- [14] M. Leyrie, G. Hervé, *Nouv. J. Chim.* **1978**, *2*, 233-237.
- [15] F. Robert, M. Leyrie, G. Hervé, A. Tézé, Y. Jeannin, *Inorg. Chem.* **1980**, *19*, 1746-1752.
- [16] M. Leyrie, R. Thouvenot, A. Tézé, G. Hervé, *New J. Chem.* **1992**, *16*, 475-481.
- [17] Y. Jeannin, J. Martin-Frère, *Inorg. Chem.* **1979**, *18*, 3010-3014.
- [18] W. G. Klemperer, G. Westwood, *Nature Materials (News & Views)* **2003**, *2*, 780-781.
- [19] K. Wassermann, M. T. Pope, *Inorg. Chem.* **2001**, *40*, 2763-2768.
- [20] **Preparation of 6:** To a solution of the sodium salt of **2a** (1.5 g) (prepared according to reference [17]) in 40 mL of H₂O which was adjusted to pH=1.9 with 2 mL 0.5M H₂SO₄ VOSO₄ · 5H₂O (2 g, 8 mmol) was added. The solution was stirred at room temperature for 24h, and then heated to 70-80 °C. After addition of NH₄Cl (3.5 g, 65.38 mmol) the solution was kept at this temperature for 30 min and then filtered hot. After 12 days the precipitated dark-brown crystals of **6** were filtered. Yield 0.4 g (24% based on W). Elemental analysis calcd (%) for H₁₇₀As₄N₂₂O₁₈₄V₃W₄₀ (11229.5): N 2.7, V 1.3; found: N 2.5, V 1.2.

Unit cell parameters for **6**: $a = 50.064(3)$, $b = 19.8450(10)$,
 $c = 39.185(2)$ Å, $\beta = 110.50(1)^\circ$, $V = 36465(3)$ Å³;
monoclinic space group $P2_1/c$ (for the magneto-chemical
characterisation see text).

[21] S. P. Harmalker, M. A. Leparulo, M. T. Pope, *J. Am. Chem. Soc.* **1983**, *105*, 4286-4292.

[22] J. R. Pilbrow, *Transition Ion Electron Paramagnetic Resonance*, Clarendon, Oxford, **1990**.

[23] O. Kahn, *Molecular Magnetism*, VCH, New York, **1993**.

[24] Y. H. Cho, Ph. D. Thesis, *Single Crystal EPR Studies on Magnetic Interactions in Polyoxometalates Containing Several Paramagnetic Ions*, Sogang University, Seoul, **1996**.

[25] K.-C. Kim, M. T. Pope, *J. Chem. Soc., Dalton Trans.* **2001**, 986-990.

[26] J.-F. Liu, Y.-G. Chen, L. Meng, J. Guo, Y. Liu, M. T. Pope, *Polyhedron* **1998**, *17*, 1541-1546.

[27] Y. H. Cho, H. So, M. T. Pope in *Modern Applications of EPR/ESR: From Biophysics to Materials Science* (Proc. First Asia-Pacific EPR/ESR Symposium) (Eds.: C. Z. Rudowicz, K. N. Yu, H. Hiraoka), Springer, Singapore, **1998**, pp. 202-209.

[28] a) A. Müller, S. K. Das, S. Talismanov, S. Roy, E. Beckmann, H. Bögge, M. Schmidtman, A. Merca, A. Berkle, L. Allouche, Y. Zhou, L. Zhang, *Angew. Chem.* **2003**, *115*, 5193-5198; *Angew. Chem. Int. Ed.* **2003**, *42*, 5039-5044; b) A.

Müller, E. Krickemeyer, H. Bögge, M. Schmidtman, B. Botar, M. O. Talismanova, *Angew. Chem.* **2003**, *115*, 2131-2136; *Angew. Chem. Int. Ed.* **2003**, *42*, 2085-2090.

[29] According to a nice description in reference [18] the cryptand type can be described as follows: the "[...] polyoxoanion has an annular structure, with a central cation binding site surrounded by four equivalent binding sites arranged on its interior surface. In this arrangement, a "large" central cavity similar to a very distorted cube of eight oxygen atoms is formed, whereas each of the four smaller binding sites has square pyramidal geometry defined by four basal oxygen atoms and an apical arsenic atom [...]".

[30] The treatment of an aqueous solution of **1** with a trichlormethane solution of DODA^+Br^- leads to a transfer of the complex anion **1a** into the organic phase. Related studies are in progress. For similar encapsulation studies of the giant spherical cluster anions mentioned in the introduction see: a) D. G. Kurth, P. Lehmann, D. Volkmer, H. Cölfen, M. J. Koop, A. Müller, A. Du Chesne, *Chem. Eur. J.* **2000**, *6*, 385-393; b) D. Volkmer, A. Du Chesne, D. G. Kurth, H. Schnablegger, P. Lehmann, M. J. Koop, A. Müller, *J. Am. Chem. Soc.* **2000**, *122*, 1995-1998; c) D. G. Kurth, D. Volkmer, M. Ruttorf, B. Richter, A. Müller, *Chem. Mater.*

2000, 12, 2829-2831; d) D. G. Kurth, P. Lehmann, D. Volkmer, A. Müller, D. Schwahn, *J. Chem. Soc., Dalton Trans.* 2000, 3989-3998; e) F. Caruso, D. G. Kurth, D. Volkmer, M. J. Koop, A. Müller, *Langmuir* 1998, 14, 3462-3465.

Legends to Figures

Figure 1. (a): Packing of the cluster anions **1a** (see Figure 1b) in the crystal lattice of **1**. Each anion is "connected" to two neighbouring anions by disordered $\text{Na}(\text{H}_2\text{O})_3$ units forming infinite chains parallel to the crystallographic c axis (top to bottom). Parallel chains are rotated relative to neighbouring chains by 180° parallel to the c axis, translated by $c/2$ and then connected through additional "Na-O bonds" forming a layer-type structure (colour code as in Figure 1b; Na^+ ions shown as grey spheres coordinating H_2O molecules as red spheres). (b) and (c): Structure of **1a** (b) (in polyhedral representation) and comparison with that of **4a**, **5a** (c) (in polyhedral and schematic representation; S1, S2 and S2' denoted as in reference [15]). All three anions are built up by four AsM_9 -type units (green polyhedra, with As centres as orange spheres) linked by four WO_6 octahedra (light green polyhedra). In **1a** (b) two tungsten positions in two of the four AsM_9 units (top and bottom) are partially occupied by vanadium atoms (related polyhedra blue). Three additional vanadium centres occupy the sites marked as S1 and S2 in Figure 1c. A $\text{VO}_5(\text{H}_2\text{O})$ octahedron fills position S1, while two OVO_4 square pyramids

occupy the S2 positions . The S2' sites are formally "filled" by SO_4^{2-} tetrahedra while the AsM_9 (i.e. V/W) and SO_4^{2-} units have O atoms in common. (The colour code for the polyhedra and the O atoms is chosen to illustrate the formal building blocks as given in the formula of **1**: " $\text{V}^{\text{IV}}\text{O}(\text{H}_2\text{O})$ " red octahedron with two yellow spheres; " $\text{V}^{\text{IV}}\text{O}$ " red square pyramids with one yellow sphere; " SO_4 " yellow tetrahedra with four red spheres; " WO_2 " light green polyhedra with two green spheres). In **4a** (c) the S1 and S2' positions are occupied by NH_4^+ cations, and both S2 sites by Co^{2+} . In **5a** (c) all S1, S2 and S2' sites are occupied by Na^+ cations; chloride anions bridge the Na^+ cations in the S2 and S2' sites (see reference [19]).

Figure 2. (a): Side view of **1a** highlighting the cavity with the interatomic distances [\AA] corresponding to short hydrogen bonds between the sulphate groups and the central $\text{V}^{\text{IV}}\text{O}_5(\text{H}_2\text{O})$ octahedron. (b): The interatomic distances [\AA] and angles [$^\circ$] between the three V^{IV} centres inside the cavity of **1a** defining a triangle (colour code as in Figure 1).

Figure 3. The molar susceptibility temperature product versus temperature for **1**, recorded on a powder sample at an 0.5 T applied field.

Figure 4. The molar susceptibility - temperature product versus temperature for **6** (squares). The drawn line is a fit assuming a linear triangular cluster of three $S = \frac{1}{2}$ ions, without exchange interactions between the outer ions.

Table of Contents

Replacing some of the internal W atoms of the $\{\text{As}_4\text{W}_{40}\text{O}_{140}\}$ -type cryptand by V atoms leads to a higher reactivity of the internal cavity shell; this allows a new type of *encapsulation chemistry under confined conditions* for anions and cations.

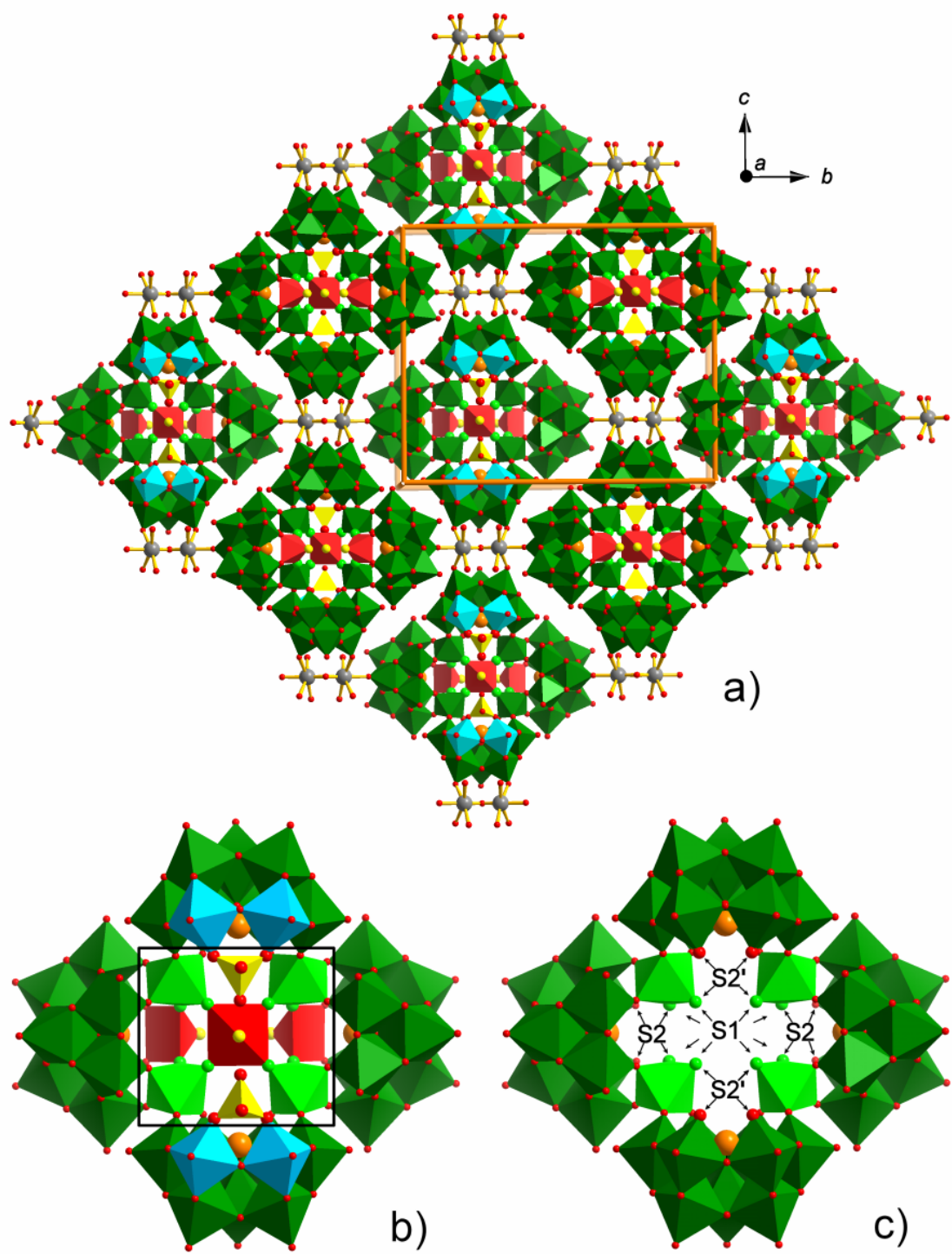
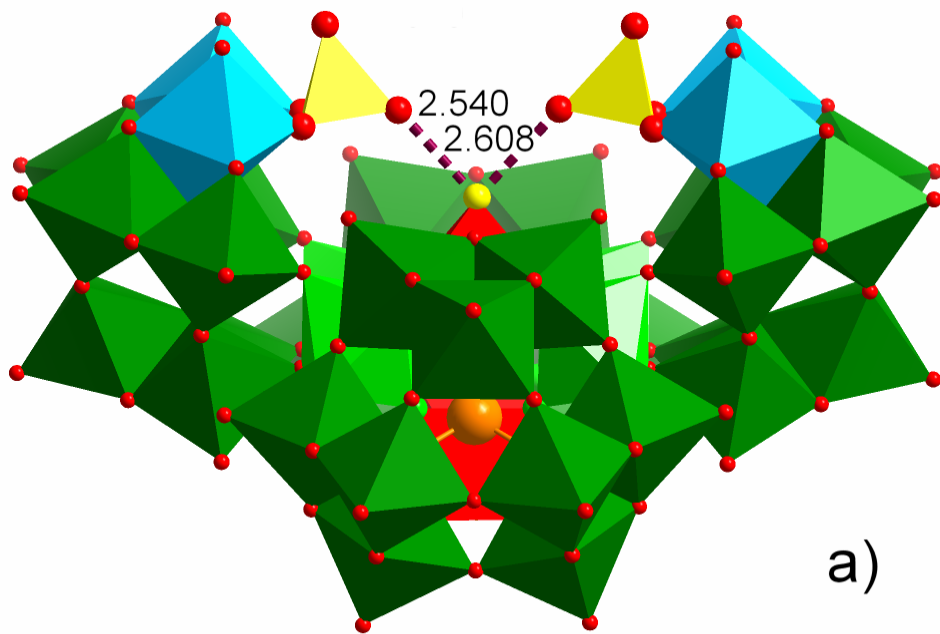
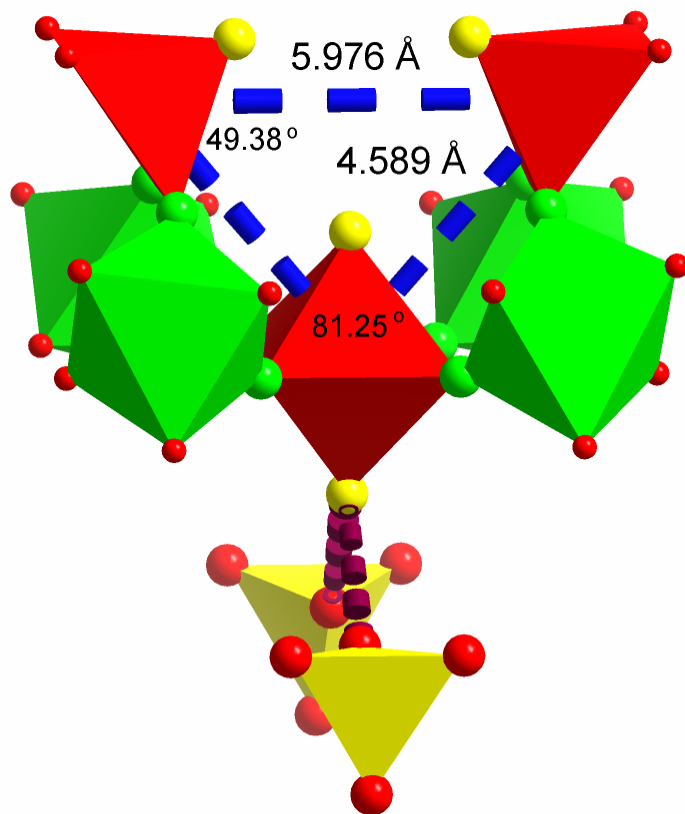


Figure 1.



a)



b)

Figure 2.

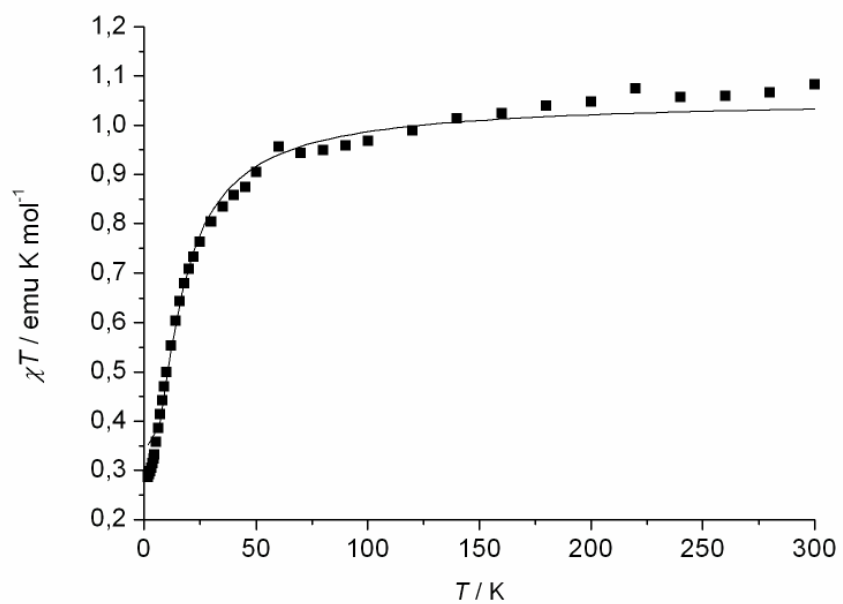


Figure 3.

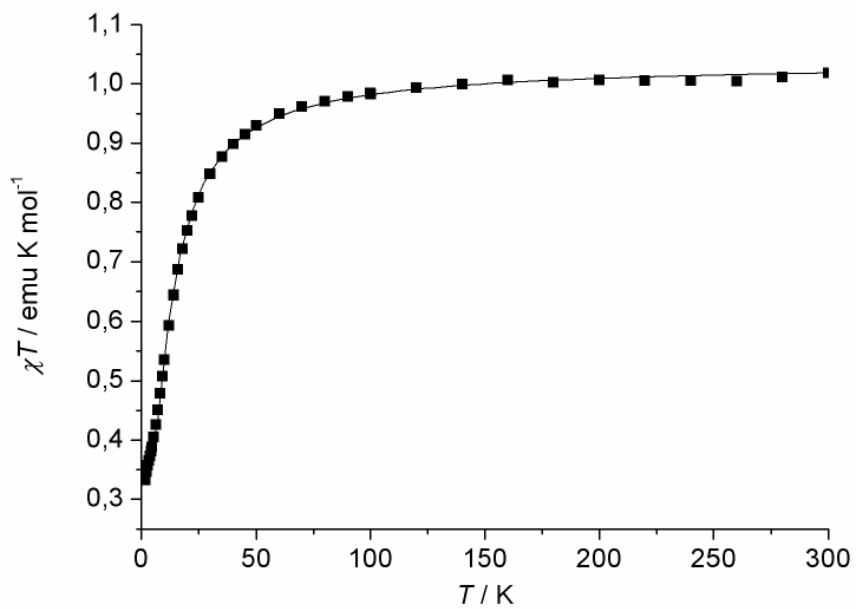


Figure 4.

"Nano-ion Chromatograph"

Trapping Cations in Specific Positions in Tuneable
"Artificial Cell" Channels: New Nanochemistry
Perspectives**

Achim Müller,* Samar K. Das, Sergei Talismanov,
Soumyajit Roy, Eike Beckmann, Hartmut Bögge,
Marc Schmidtman, Alice Merca, Alois Berkle,
Lionel Allouche, Yunshan Zhou, and Lijuan Zhang

Dedicated to Professor Ram Rao
on the occasion of his 70th birthday

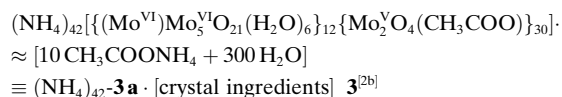
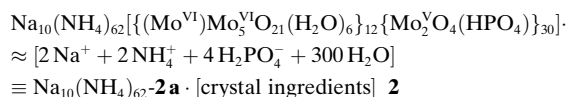
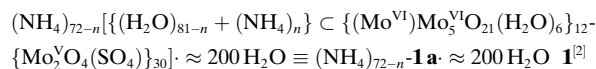
Molecular dimensioned holes can serve as filters but also trap molecules with well-defined shapes. Whereas a large number of porous materials with cages and tunnels exist as extended structures,^[1] as yet not much is known about well-defined, discrete (molecular) nanoporous species. Processes that refer to the entrance of substrates (e.g. of cations) are of particular interest if the affinity of *specific* substrates to *specific* capsule areas can be predicted. This is now possible for nanosized spherical capsules based on the robust fundamental skeleton (pent)₁₂(linker)₃₀≅{(Mo)Mo₅O₂₁(H₂O)₆}{Mo₂O₄(ligand)}₃₀^[2,3] which has sizeable pores, finely sculpturable interiors and, in between, tuneable functionalized channels with unprecedented molecular-scale filter properties. These will be discussed here for the first time. Most importantly, the channel functionalities as well as the capsule size and charge can be extensively varied, while charge modulations lead to related changes in the affinity to cations! Herein we show that different substrates/cations can be fixed at well-defined positions above, below, and especially in the channels.^[3] This situation allows us to study, in principle, new types of molecular transport phenomena, including osmotic-type ones, on the nanoscale, and shows properties of a "nano-ion chromatograph".^[4] Additionally, one can construct new geometries such as interpenetrating solids from entering cations owing to the fact that we have a multitude of different as well as equivalent sites in the channels, pores, and in the interior (see also ref. [3b]). This also allows us to study properties of matter under confined conditions.

For the investigations into the uptake of cations and substrates, we used the known capsule **1a**^[3] as well as the new

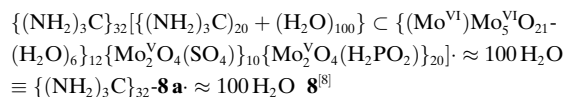
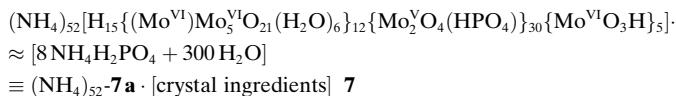
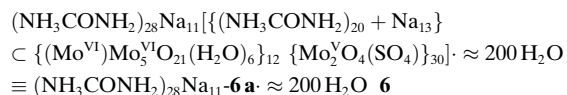
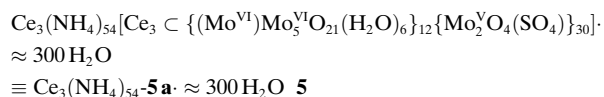
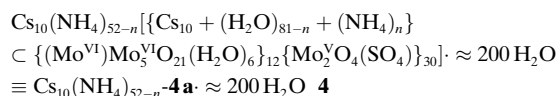
[*] Prof. Dr. A. Müller, Dr. S. K. Das, Dr. S. Talismanov, S. Roy, E. Beckmann, Dr. H. Bögge, M. Schmidtman, A. Merca, A. Berkle, Dr. L. Allouche, Dr. Y. Zhou, Dr. L. Zhang
Lehrstuhl für Anorganische Chemie I
Fakultät für Chemie der Universität
Postfach 100131, 33501 Bielefeld (Germany)
Fax: (+49) 521-106-6003
E-mail: a.mueller@uni-bielefeld.de

[**] The authors gratefully acknowledge the financial support of the Deutsche Forschungsgemeinschaft, the Fonds der Chemischen Industrie, and the Volkswagen Stiftung. S.R. and A.M. thank the "Graduiertenkolleg Strukturbildungsprozesse", Universität Bielefeld, for their fellowships and L.A. thanks the European Union for a grant (HRPN-CT-1999-0012).

capsule **2a**^[5] (both can be easily obtained from **3a**; see Experimental Section) that exhibits the above-mentioned skeleton. As they contain the neutral linker units {Mo₂O₄(SO₄)} and {Mo₂O₄(HPO₄)}, the overall cluster charge corresponds to that of the 12 pentagonal units, that is, 12 × (6−) = 72−.



The reaction of **1a** and **2a** with different substrates/cations such as Na⁺, Cs⁺, Ce³⁺, and OC(NH₂)NH₃⁺ in aqueous solution leads to the formation of compounds **4–7**, respectively, which exhibit well-defined cation separations at, above, or below the capsule's channel-landscapes (“nano-ion chromatography” principle). All compounds were characterized in the solid state by elemental analyses, thermogravimetry (to determine the amount of water of crystallization), single-crystal X-ray diffraction analyses^[6] (including bond valence sum (BVS) calculations), IR spectroscopy,^[7a] and ³¹P solid-state NMR^[7b] studies.



Whereas the basic skeleton {(Mo)Mo₅O₂₁(H₂O)₆}{Mo₂O₄(ligand)}₃₀ of the capsule of the precursors **1a** (see refs [2,3]) and **2a** and of the resulting species **4a–7a** is the same, **4a–7a** show after cation uptake the expected different interiors (Figure 1, 2); this is a situation for molecular materials never observed before. The uptake leads to stoichiometric preferences when the cations are fixed in the higher channel areas, that is, if the {Mo₉O₉} pores can function like a type of crown ether. Non-stoichiometric situations can

also occur there, but especially below the pore area. In these cases the uptake can be increased by increasing related concentrations and the capsule charge. Whereas the large, stoichiometrically bound, protonated urea cations in **6a** fit reasonably well into the {Mo₉O₉} rings/pores (see below), the somewhat smaller Cs⁺ ions are not found exactly at the pore centers, but slightly shifted. The even smaller Rb⁺ ions show complicated “chameleonic” behavior and are found at several different capsule functionalities, including positions outside the capsule, as there are no characteristic complementary sites available: the Rb⁺ ion is too small to be fixed inside the {Mo₉O₉} rings and seems to be too large to enter into the channels (see Figure 1). Finally, the much smaller Ce³⁺ ions can enter easily into the capsule interior through the whole channel areas as in **5a**. Comparing the Ce³⁺ behavior with that of Na⁺ is especially instructive: Na⁺ ions are trapped within the lower part of the channels as they fit exactly into a well-defined site spanned by three oxygen atoms of three SO₄^{2−} ligands (Figure 1 and 2); on the other hand, Ce³⁺ ions are found below the channels and each is coordinated symmetrically in a bidentate fashion to only one SO₄^{2−} ligand. The 30 equivalent Ce³⁺-type positions span an icosidodecahedron (see below). Importantly, the protonated urea cations in **6a** and also the guanidinium cations in **8a**^[8] are noncovalently coordinated to the oxygen atoms of the {Mo₉O₉} pores through hydrogen bonds in the usual way known in supramolecular chemistry;^[9] a guanidinium cation analogue based on a crown-ether structure has already been described.^[9]

The channels of the clusters are lined with nucleophilic/hydrophilic chemical groups conducive to the passage of electrophilic (i.e., positively charged) ions.^[10] Ligands such as sulfate and phosphate promote cation diffusion leading to selectivity and mechanisms controlling the flux. There is also the option of different substrates coordinating simultaneously in the higher and lower parts of the “channels” along the C₃ axes in the direction of the capsule center if the cations are simultaneously present. This offers, in principle, also the possibility to study novel types of cooperativity interactions between different types of encapsulated, fixed cationic centers including paramagnetic ones. When the usual reaction system forming **1a**^[2a] is treated with a strong electrolyte solution, such as NaCl in the presence of urea, the cluster anion **1a** “takes up” Na⁺ ions before channel “closing” with protonated urea, and forming **6a**. This remarkable preferential trafficking depends specifically on the activity of different functional groups of the capsule.

As the channels’ “clothes” can be modified by exchanging ligands attached to the 30 linkers the option exists to use different related functionalities. This is nicely demonstrated by the reaction of **3a** with phosphate ions at different pH values. At about pH 5, the acetate groups are replaced by phosphate groups leading to the formation of **2a**. But if the same reaction is performed at a lower pH (ca. 2; which leads to a partial decomposition of **2a**, that is, with some “molybdate formation”), a novel type of cavity-internal reaction occurs: a nucleation process between the phosphate ligands and the molybdate—released through the preceding reaction—takes place below the {Mo₉O₉} rings by linking {MoO₃H} groups to phosphate ligands under formation of

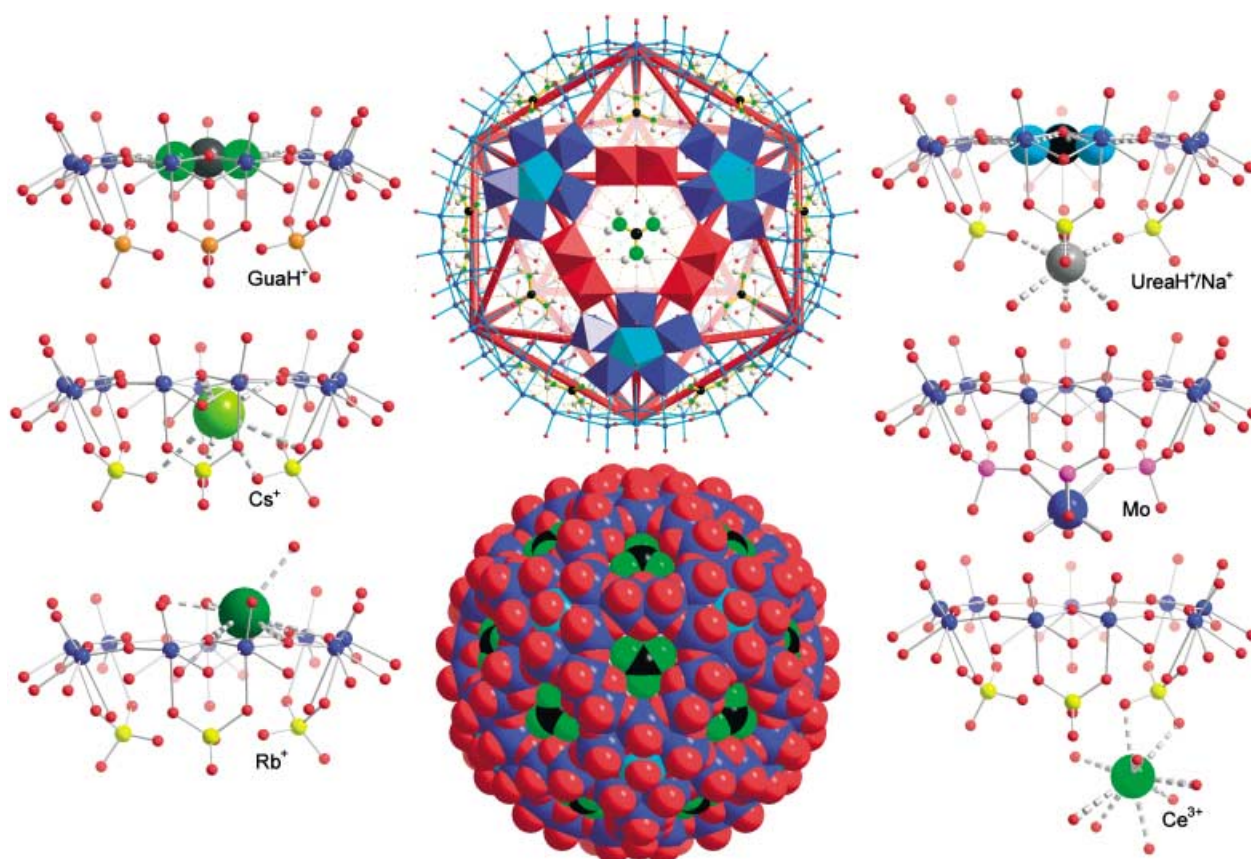


Figure 1. Cations residing at well-defined positions of the capsule of the type $\{[(\text{Mo})\text{Mo}_5\text{O}_{21}(\text{H}_2\text{O})_6]_{12}[\text{Mo}_2\text{O}_4(\text{ligand})]_{30}\}$ with 20 pores and channels. Bottom middle: one whole capsule with guanidinium guests (space-filling); top middle: the main entering portion of one of the 20 $\{\text{Mo}_9\text{O}_9\}$ pores (with a guanidinium guest) placed on one of the 20 faces of the icosahedron spanned by the 12 central Mo atoms of the pentagonal units in polyhedral representation (see also ref. [3a]). Left and right rows: within the $\{\text{Mo}_9\text{O}_9\}$ rings/pores the protonated urea (**6a**, top right) and guanidinium cations (**8a**, top left), below, Na^+ within a channel in an environment spanned by three O atoms of three sulfate ligands (**6a**, top right), further below three O atoms of the related phosphate ligands that “fix” the Mo atom of the $\{\text{MoO}_3\text{H}\}$ group (**7a**, middle right); whereas the rather large Cs^+ ions are found approximately in the pore centers (**4a**, middle left), the small Ce^{3+} ions are positioned below the channels (**5a**, bottom right). As no specific positions are available for Rb^+ ions, these are found in a complicated distribution (only one of which is shown) at several positions even outside the capsule (bottom left). Color code: Mo blue, O red, S yellow, P violet, P/S (of **8**) brown, C black, N green; other respective substrates/cations in different colors.

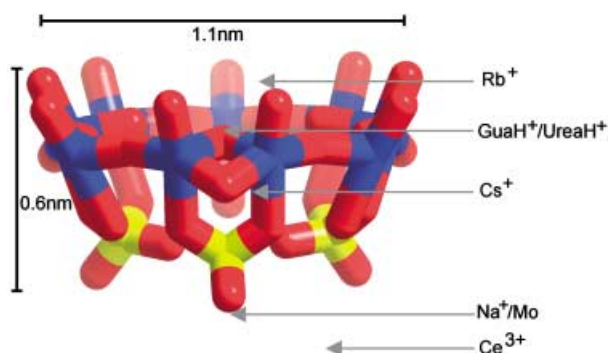


Figure 2. The relative positions of all the fixed substrates in one of the 20 channels (wire-frame representation; color code as in Figure 1).

7a.^[11] As geometric constraints allow only for accommodation of up to eight $\{\text{MoO}_3\text{H}\}$ moieties exactly positioned at the C_3 axes (but according to the underoccupation only five $\{\text{MoO}_3\text{H}\}$ groups are found), this leads to the generation of a new type of interpenetrating solids in a confined spherical

geometry: a cube spanned by eight characteristic $\{\text{MoO}_3\text{H}\}$ -type positions inscribed within a dodecahedron (Figure 3; see also ref. [3b]). The reaction would not occur in case of **1a** with the sulfate channel type, since the relevant anion has a lower electron density at the O atoms and therefore a lower affinity to protonation which is a necessary precondition for a condensation process.

Summary and perspectives: Our capsules can be considered as nanoscale laboratories^[12] with a variety of functionalities that enable the positioning of substrates/cations under controlled conditions. Additionally, cation trapping in the 20 pores and channels can be achieved stepwise and several times, respectively, with the consequence that the affinity of the positive substrates to the sites of the negative capsule changes with each cation trapping event due to the decrease of negative charge, a phenomenon which can be regarded as one of the hallmarks of nanotechnology. Interestingly, also capsules with relatively small charges (like that of **3a**) may attract cations, provided that they have a larger charge than the monovalent ones mentioned above: $[\text{M}(\text{H}_2\text{O})_6]^{2+}$ ($\text{M} =$

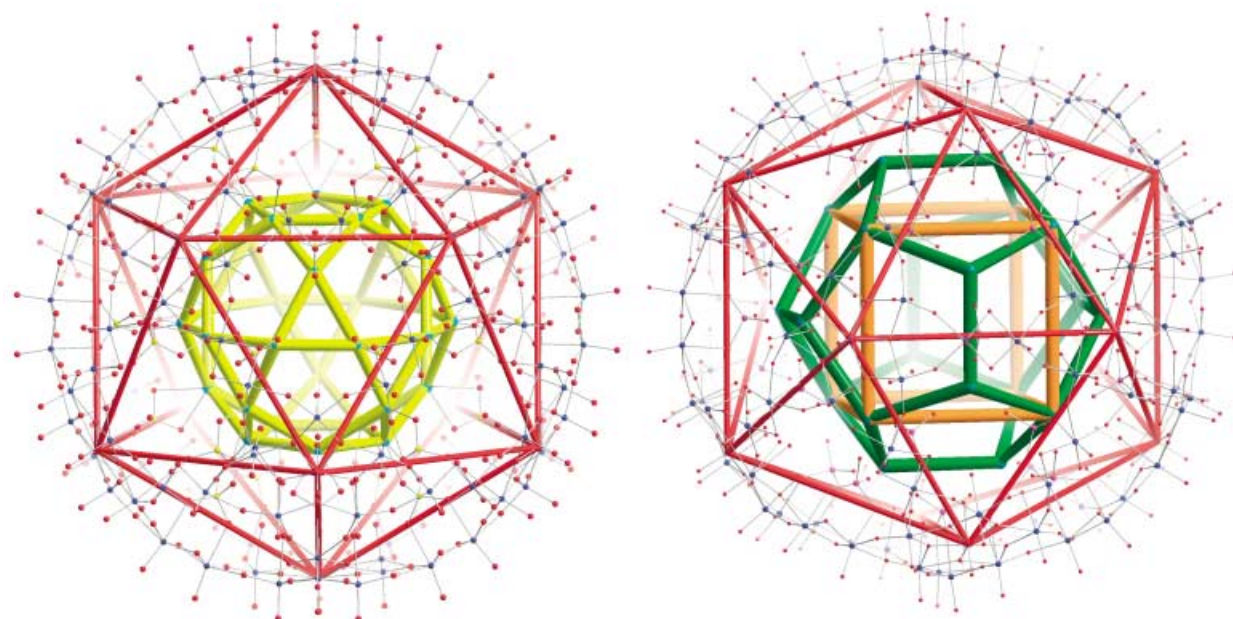


Figure 3. Interpenetrating solids within the capsules of **5 a** and **7 a** (ball-and-stick model; color code as in Figure 1). Right: a cube (orange) with eight (possible) $\{\text{MoO}_3\text{H}\}$ -type positions as part of the 20 vertices of a dodecahedron (green) spanned by all 20 symmetry-related channel positions on the C_3 axes in **7 a** (see also ref. [3b]); left: an icosidodecahedron (yellow) formed by the characteristic Ce^{3+} ion positions of **5 a** which are related here to the icosahedron (red) spanned by the 12 central Mo atoms of the pentagonal units—deliberately shown in spite of underoccupation to demonstrate the option of generating different interpenetrating solids.

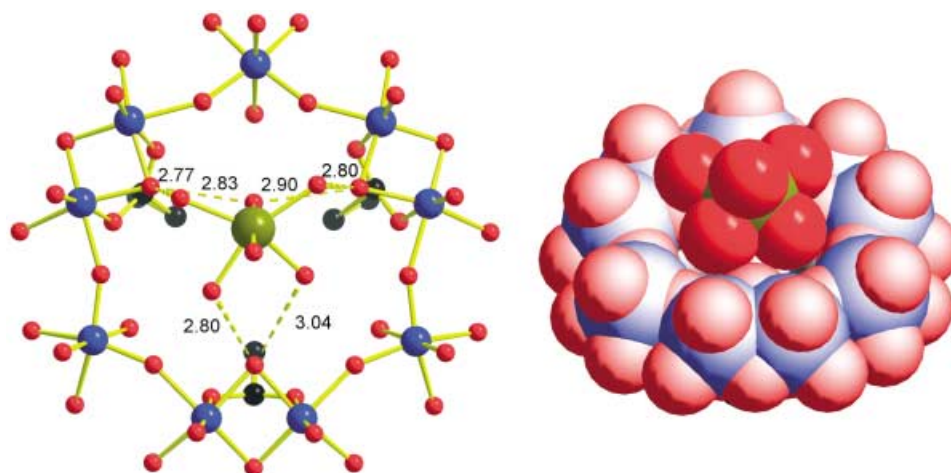


Figure 4. Ball-and-stick (with distances (Å), left) and space-filling representation (right) of one of the $[\text{Ni}(\text{H}_2\text{O})_6]^{2+}$ complexes interacting through hydrogen bonds with one of the $\{\text{Mo}_9\text{O}_9\}$ pores of the acetate-type capsule **3 a**, leading to the formation of a novel supramolecular cluster arrangement (in the compound about 16 of the 42NH_4^+ ions of **3 a** are replaced by the Ni units; color code as in Figure 1, Ni olive green).

Mg, Ca, Ni) complexes in solution^[13] are attracted and fixed through formation of hydrogen bonds between their H_2O ligands and the O atoms in the capsule pores^[14] (see Figure 4, which also shows relevant distances). The Ni–O–H \cdots O interactions, that is, second-sphere coordinations, might be considered as an interesting supramolecular cluster phenomenon with perspectives for further investigations.^[14] Importantly, the separation of cations in aqueous solution allows, in principle, the option of fabricating a “nano-ion chromatograph”, as the “artificial cells” respond to their solute/solvent environment in a specific way. For instance, well-defined, hydrated metal ions such as the above complexes are blocked

by the pores because of their size. As the reactions are performed under the conditions of nanocapsule confinement while the capsule size and charge can be precisely generated, new and basic processes may emerge that need not necessarily agree with those observed in bulk materials though also offering new insight into related bulk reactions. For example, it was found very recently that at least five water molecules were necessary to observe dissociation of HBr.^[15] Our systems can, generally speaking, provide insight into the influence of geometric confinement on different substrate positionings but especially allow—because of the multitude of different types of equivalent sites—the generation of novel nanoscopic

architectures, for example, with interpenetrating solids like a cube in a dodecahedron (see Figure 3 and refs. [3b,11]).

Experimental Section

3: Compound **3** was prepared as reported in ref. [5].

2: Compound **3** (3.0 g, 0.11 mmol) was added under constant stirring to a solution of NaH_2PO_4 (3 g, 25 mmol) and NH_4Cl (3 g, 56 mmol) in H_2O (200 mL). The pH was adjusted to ~ 5 with NH_4OH . The red-brown crystals that precipitated from the solution after five days were filtered off and dried at room temperature. Yield: 1.5 g. Elemental analyses (%) calcd: Na 0.9, N 3.1, P 3.6; found: Na 0.8, N 3.0, P 3.6.

4: A solution of **3** (4.0 g, 0.14 mmol) in H_2O (350 mL) was treated with cesium sulfate (16.5 g, 45.6 mmol) and was stirred at 80°C for 3 h. The resulting reaction mixture was kept at room temperature for 24 h. The precipitated microcrystalline solid was filtered, washed with water, and dried at room temperature. After the solid was suspended in an ammonium sulfate solution (10.0 g in 350 mL), the suspension was heated at 80°C for 10–12 min, whereby a clear solution was obtained. The solution was filtered and kept at room temperature for one week in an open 1 L beaker, and red-brown crystals of **4** precipitated. To obtain “better” crystals, the precipitate was redissolved by subsequent warming on a hot plate at $70\text{--}80^\circ\text{C}$ in the same mother liquor by adding water (130 mL), and the resulting clear solution was kept in the same open beaker for one week. The precipitated brown rhombohedral crystals, which are more suitable for a structure determination than the first precipitated crystals crystallizing in the cubic space group showing a problematical disorder, were filtered, washed with 2-propanol, and dried at room temperature. Yield: 2.1 g. Elemental analyses (%) calcd: Cs 8.7, N 2.4, S 3.1; found: Cs 8.7, N 2.5, S 3.4.

5: $\text{CeCl}_3 \cdot 7\text{H}_2\text{O}$ (10.0 g, 26.8 mmol) was added after 1.5 h to a refluxing solution of **3** (5.0 g, 0.18 mmol) and ammonium sulfate (15.0 g, 113.5 mmol) in H_2O (400 mL). The resulting solution was refluxed for 30 min and filtered hot. The dark brown crystals of **4** that precipitated after one day were filtered, washed with ice-cold 2-propanol, and dried in air. Yield: 4.4 g. Elemental analyses (%) calcd: Ce 2.9, N 2.6, S 3.2; found: Ce 2.6, N 3.0, S 3.6.

6: A mixture of **3** (0.5 g, 0.02 mmol), urea (1.0 g, 16.7 mmol), $(\text{NH}_4)_2\text{SO}_4$ (2.5 g, 18.9 mmol), H_2O (40 mL), and 16% HCl (8 mL) in a 100-mL Erlenmeyer flask (covered with a watch-glass) was heated to $60\text{--}70^\circ\text{C}$. After 90 min, NaCl (3.0 g, 51.3 mmol) was added and the solution was heated for 90 min and then kept at room temperature. After 3–4 days brown rhombohedral crystals of **6** were filtered off, washed with a small amount of ice-cold water, then with ice-cold 2-propanol, and dried in air. Yield: 0.35 g. Elemental analyses (%) calcd: Na 1.9, C 1.9, N 4.6; found: Na 2.1, C 1.8, N 4.6.

7: Compound **3** (3.0 g, 0.11 mmol) was added under constant stirring (15 min) to a solution of $\text{NH}_4\text{H}_2\text{PO}_4$ (3 g, 26 mmol), NH_4Cl (3 g, 56 mmol) and HCl (15 mL, 1M) in H_2O (200 mL). After the solution was kept in an open beaker at room temperature for seven days, the precipitated red-brown crystals of **7** were filtered off and dried at room temperature. Yield: 2.0 g. Elemental analyses (%) calcd: N 2.8, P 3.9; found: N 2.8, P 3.9.

The chemical formulas refer to the maximum number of water molecules in the crystal, which is in agreement with the cell volume. According to the observed loss of water the analytical data, however, refer to this number of crystal water molecules minus 50.

Received: July 11, 2003 [Z52358]

Published Online: October 8, 2003

Keywords: confined geometries · encapsulation · ion transport/uptake · nanotechnology · porous materials

- [1] a) *Handbook of Porous Solids* (Eds.: F. Schüth, K. S. W. Sing, J. Weitkamp), Wiley-VCH, Weinheim, **2002**; b) M. A. White, *Properties of Materials*, Oxford University Press, New York, **1999**, chap.: Inclusion Compounds; c) G. Férey, *Science* **2001**, *291*, 994–995.
- [2] a) A. Müller, E. Krickemeyer, H. Bögge, M. Schmidtman, B. Botar, M. O. Talismanova, *Angew. Chem.* **2003**, *115*, 2131–2136; *Angew. Chem. Int. Ed.* **2003**, *42*, 2085–2090; b) A. Müller, E. Krickemeyer, H. Bögge, M. Schmidtman, F. Peters, *Angew. Chem.* **1998**, *110*, 3567–3571; *Angew. Chem. Int. Ed.* **1998**, *37*, 3360–3363.
- [3] a) A. Müller, P. Kögerler, C. Kuhlmann, *Chem. Commun.* **1999**, 1347–1358; b) A. Müller, *Science* **2003**, *300*, 749–750. c) The term stability refers here to the fact that at least in the final product always the same type of well-defined capsules are found with the expected functionalities after reactions have taken place in solution. But, in principle, it cannot be excluded that in solution the pores, that is, the $\{\text{Mo}_9\text{O}_9\}$ rings, are opened slightly during uptake. Related solution NMR studies concerning the stability and reaction pathways are currently possible and are in progress (F. Taulelle, M. Henry, A. Müller; see also ref. [5]).^[16]
- [4] See also related discussion in: M. Gross, *Chem. Br.* **2003**, *39* (August Issue), p. 18. As the cations entering through the gates are not randomly distributed in the cell interior but fixed at functionalities according to their specific properties, thus relatively reducing the whole capsule system entropy, a situation results that is formally comparable to that of “Maxwell’s Demon”, but acting in a closed system (the related Gedanken experiment is for instance explained in textbooks of Statistical Thermodynamics and even in *The New Encyclopaedia Britannica*, Vol. 23, 15th ed., Encyclopaedia Britannica, Chicago, **2002**, p. 692, including the statement: “The hypothetical intelligent being known as Maxwell’s demon was a factor in the development of information theory”). See also: M. Gross, *Travels to the Nanoworld: Miniature Machinery in Nature and Technology*, Perseus Publishing, Cambridge, Massachusetts, **2001** (Chapter: Maxwell’s demon—a predecessor of nanotechnology?); D. E. H. Jones, *Nature* **1995**, *374*, 835–837.
- [5] Both are formed by ligand exchange from **3a**, which is available in facile syntheses according to: L. Cronin, E. Diemann, A. Müller in *Inorganic Experiments* (Ed.: J. D. Woollins), 2nd ed., Wiley-VCH, Weinheim, **2003**, pp. 340–346 and A. Müller, S. K. Das, E. Krickemeyer, C. Kuhlmann, *Inorg. Synth.* **2003**, *34*, in press. The sulfate cluster anion $\mathbf{1a}^{[2a]}$ with the high charge of 72– is formed from **3a** in situ in solution during the processes leading to **4a**, **5a**, and **6a**, which can also be obtained by starting from solutions of crystalline **1**. Important in context with footnote [3] is that **1a** can be obtained by ligand exchange from **3a** without heating, that is at room temperature and under low pH conditions which supports the release of the leaving group acetic acid.
- [6] Crystal data for **2**: $\text{H}_{1038}\text{Mo}_{132}\text{N}_{64}\text{Na}_{12}\text{O}_{880}\text{P}_{34}$, $M_r = 30015.89 \text{ g mol}^{-1}$, cubic space group $Fm\bar{3}$, $a = 45.6162(12) \text{ \AA}$, $V = 94920(4) \text{ \AA}^3$, $Z = 4$, $\rho = 2.100 \text{ g cm}^{-3}$, $\mu = 1.862 \text{ mm}^{-1}$, $F(000) = 58848$, crystal size = $0.24 \times 0.24 \times 0.24 \text{ mm}^3$. A total of 120764 reflections ($0.77 < \theta < 25.02^\circ$) were collected, of which 7311 reflections were unique ($R(\text{int}) = 0.0578$). $R = 0.0832$ for 4974 reflections with $I > 2\sigma(I)$, $R = 0.1464$ for all reflections, max./min. residual electron density 1.316 and $-1.715 \text{ e \AA}^{-3}$. Crystal data for **4**: $\text{H}_{914}\text{Cs}_{20}\text{Mo}_{132}\text{N}_{52}\text{O}_{845}\text{S}_{30}$, $M_r = 31453.91 \text{ g mol}^{-1}$, rhombohedral space group $R\bar{3}$, $a = 32.7258(8)$, $c = 73.664(3) \text{ \AA}$, $V = 68323(3) \text{ \AA}^3$, $Z = 3$, $\rho = 2.293 \text{ g cm}^{-3}$, $\mu = 2.725 \text{ mm}^{-1}$, $F(000) = 45486$, crystal size = $0.25 \times 0.20 \times 0.15 \text{ mm}^3$. A total of 188827 reflections ($0.77 < \theta < 30.01^\circ$) were collected, of which 44291 reflections were unique ($R(\text{int}) = 0.0564$). $R = 0.0498$ for 32184 reflections with

$I > 2\sigma(I)$, $R = 0.0789$ for all reflections, max./min. residual electron density 2.369 and $-1.403 \text{ e \AA}^{-3}$. Crystal data for **5**: $\text{H}_{960}\text{Ce}_6\text{Mo}_{132}\text{N}_{54}\text{O}_{864}\text{S}_{30}$, $M_r = 30014.82 \text{ g mol}^{-1}$, rhombohedral space group $R\bar{3}$, $a = 32.7411(7)$, $c = 73.682(2) \text{ \AA}$, $V = 68404(3) \text{ \AA}^3$, $Z = 3$, $\rho = 2.186 \text{ g cm}^{-3}$, $\mu = 2.229 \text{ mm}^{-1}$, $F(000) = 43866$, crystal size $= 0.40 \times 0.25 \times 0.20 \text{ mm}^3$. A total of 136090 reflections ($0.77 < \theta < 27.02^\circ$) were collected, of which 33123 reflections were unique ($R(\text{int}) = 0.0277$). $R = 0.0424$ for 27495 reflections with $I > 2\sigma(I)$, $R = 0.0559$ for all reflections, max./min. residual electron density 2.242 and $-1.215 \text{ e \AA}^{-3}$. Crystal data for **6**: $\text{C}_{48}\text{H}_{784}\text{Mo}_{132}\text{N}_{96}\text{Na}_{24}\text{O}_{812}\text{S}_{30}$, $M_r = 29881.35 \text{ g mol}^{-1}$, rhombohedral space group $R\bar{3}$, $a = 32.8028(5)$, $c = 73.948(2) \text{ \AA}$, $V = 68910(2) \text{ \AA}^3$, $Z = 3$, $\rho = 2.160 \text{ g cm}^{-3}$, $\mu = 1.933 \text{ mm}^{-1}$, $F(000) = 43584$, crystal size $= 0.25 \times 0.25 \times 0.15 \text{ mm}^3$. A total of 190772 reflections ($0.77 < \theta < 30.02^\circ$) were collected, of which 44749 reflections were unique ($R(\text{int}) = 0.0358$). $R = 0.0395$ for 36437 reflections with $I > 2\sigma(I)$, $R = 0.0556$ for all reflections, max./min. residual electron density 2.527 and $-1.426 \text{ e \AA}^{-3}$. Crystal data for **7**: $\text{H}_{1050}\text{Mo}_{137}\text{N}_{60}\text{O}_{911}\text{P}_{38}$, $M_r = 30795.64 \text{ g mol}^{-1}$, cubic space group $Fm\bar{3}$, $a = 45.6587(12) \text{ \AA}$, $V = 95186(4) \text{ \AA}^3$, $Z = 4$, $\rho = 2.149 \text{ g cm}^{-3}$, $\mu = 1.925 \text{ mm}^{-1}$, $F(000) = 60328$, crystal size $= 0.24 \times 0.24 \times 0.24 \text{ mm}^3$. A total of 118119 reflections ($0.77 < \theta < 25.03^\circ$) were collected, of which 7327 reflections were unique ($R(\text{int}) = 0.0643$). $R = 0.0883$ for 5296 reflections with $I > 2\sigma(I)$, $R = 0.1371$ for all reflections, max./min. residual electron density 1.701 and $-1.782 \text{ e \AA}^{-3}$. Crystals of **2**, **4**, **5**, **6**, and **7** were removed from the mother liquor and immediately cooled to 173–193 K on a Bruker AXS SMART diffractometer (three-circle goniometer with 1 K CCD detector, $\text{MoK}\alpha$ radiation, graphite monochromator; hemisphere data collection in ω at 0.3° scan width in three runs with 606, 435, and 230 frames ($\phi = 0, 88, \text{ and } 180^\circ$) at a detector distance of 4.0–5.0 cm). For all structures empirical absorption corrections were performed by using equivalent reflections with the program SADABS 2.03. The structures were solved with the program SHELXS-97 and refined by using SHELXL-93. (SHELXS/L, SADABS from G. M. Sheldrick, University of Göttingen (Germany) **1993/97**; structure graphics with DIAMOND 2.1 from K. Brandenburg, Crystal Impact GbR, **2001**). Further details of the crystal structure investigations can be obtained from the Fachinformationszentrum Karlsruhe, 76344 Eggenstein-Leopoldshafen, Germany, (fax: (+49)7247-808-666; e-mail: crysdata@fiz.karlsruhe.de) on quoting the depository numbers CSD-413251 (**2**), CSD 413252 (**4**), CSD 413253 (**5**), CSD 413254 (**6**) and CSD 413255 (**7**).

- [7] a) Characteristic IR bands (solid, KBr pellet, $\bar{\nu}$) for compounds **1–8** due to presence of the $[(\text{Mo})\text{Mo}_5]_{12}[\text{Mo}_2]_{30}$ -type skeleton (variations $\pm 3 \text{ cm}^{-1}$): 970s, $[\nu(\text{Mo}=\text{O})]$, 860m, 800vs, 725vs, 570s; **2** shows additionally bands at 1107, 1050, 1009 $[\nu(\text{P}-\text{O})]$ and **4, 5, 6** at 1140 (m), 1035 cm^{-1} (w–m, $\nu_{\text{as}}(\text{SO}_4)$); **6** shows weak urea bands and **2, 4, 5, 7** the $\delta(\text{NH}_4)$ bands at $\approx 1400 \text{ cm}^{-1}$. b) ^{31}P MAS NMR spectra allow us to distinguish between the “phosphates” coordinated as ligands and those abundant in the crystal lattice.
- [8] A. Müller, E. Krickemeyer, H. Bögge, M. Schmidtman, S. Roy, A. Berkle, *Angew. Chem.* **2002**, *114*, 3756–3761; *Angew. Chem. Int. Ed.* **2002**, *41*, 3604–3609.
- [9] J.-M. Lehn, *Supramolecular Chemistry: Concepts and Perspectives*, VCH, Weinheim, **1995**, p. 28.
- [10] For the transport of the cations through biological membranes, negatively charged amino acids play a key role; see: D. Voet, J. G. Voet, *Biochemistry*, 2nd ed., Wiley, New York, **1995**, chap. 18.
- [11] The situation is comparable to the formation of P-O-Mo bonds during the synthesis of the $[\text{PMo}_{12}\text{O}_{40}]^{3-}$ Keggin anion at low pH values. In **7a** the phosphate ligands, instead of being positioned exactly below the $\{\text{Mo}_3\}$ groups, “are oriented” slightly towards the $\{\text{MoO}_3\text{H}\}$ group. Consequently, a $\{\text{MoO}_3\text{H}\}$ moiety is not

found in all 20 channels/sites, hence not a dodecahedron is generated by 20 $\{\text{MoO}_3\text{H}\}$ groups but “only” a cube with eight of these can be formed. (This can be visualized as only two of each of the dodecahedral pentagon vertices can be involved as sites for $\{\text{MoO}_3\text{H}\}$. As three pentagonal faces are connected at each vertex this leads to a total number of $8 = (12 \times 2)/3$ positions; see Figure 3).

- [12] For related topics see: a) K. E. Drexler, *Nanosystems: Molecular Machinery, Manufacturing, and Computation*, Wiley, New York, **1992**; b) *Recent Advances in the Chemistry of Nanomaterials* (Eds.: C. N. R. Rao, A. Müller, A. K. Cheetham), Wiley-VCH, Weinheim, in press; c) P. Ball, *Made to Measure: New Materials for the 21st Century*, Princeton University Press, Princeton, **1997**; regarding the importance of pores see also: d) J. Tersoff, *Nature* **2001**, *412*, 135–136.
- [13] D. T. Richens, *The Chemistry of Aqua Ions*, Wiley, Chichester, **1997** (Ni^{2+} has a well-defined, rather strongly bonded primary hydration sphere in aqueous solution, for example, compared to Ce^{3+}).
- [14] The phenomenon of trapping aqueous solutes/complexes will be studied separately: A. Müller, Y. Zhou, L. Zhang, L. Toma, H. Bögge, M. Schmidtman, unpublished results.
- [15] A. F. Voegelé, K. R. Liedl, *Angew. Chem.* **2003**, *115*, 2162–2164; *Angew. Chem. Int. Ed.* **2003**, *42*, 2114–2116.
- [16] **Note added in proof** (September 24, 2003): According to new NMR investigations (F. Taulelle, M. Henry, A. Müller) the stability of the capsule in solution is very high. Furthermore the exchange of the acetate ligands of the starting material **3a** is easily possible under low pH conditions (see also ref. [5]).

Artificial cell decision about metal cations entrance: the “stable” aqua complexes get trapped above the pores others slip out its water coat and the cations enter

Achim Müller,*^a Alice Merca,^a Hartmut Bögge,^a Marc Schmidtman^a and Alois Berkle^a

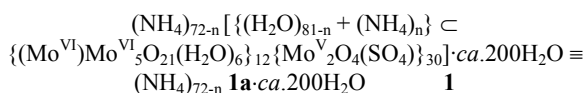
Receipt/Acceptance Data [DO NOT ALTER/DELETE THIS TEXT]

Publication data [DO NOT ALTER/DELETE THIS TEXT]

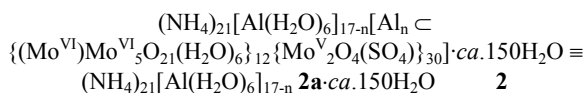
DOI: 10.1039/b000000x [DO NOT ALTER/DELETE THIS TEXT]

The highly charged unique molybdenum oxide based highly nucleophilic porous capsule exhibiting 20 nanosized pores, trap [Al(H₂O)₆]³⁺ complexes above the pores by formation of a new type of supramolecular species; the investigation of the interaction between the capsule and solutions containing hydrated metal cations allows to distinguish between complexes having strongly and less strongly bonded water molecules as ligands like between the hydrated Ni²⁺ and Mn²⁺ complexes.

In a nice small book entitled “Nanophysics and Nanotechnology”,¹ which is an introduction to modern concepts in nanoscience, in the section “Ion Channels”, the attractive aspects of the use of nanoobjects containing channels/pores is highlighted. Here we demonstrate that it is possible by using porous capsules of the type (Pentagon)₁₂(Linker)₃₀² with 20 channels connecting the 20 pores with the cavity, to distinguish between aqua ions with strongly and less strongly fixed water ligands. This type of investigation also allows the trapping of aqua complexes, which are abundant in solution, and have a rather strongly fixed hydration shell. The trapping occurs above the pores exhibiting crown ether functions, *i.e.* at well defined positions of the surface of a spherical nanoobject. Here we report on the interaction of Al³⁺ ions abundant in solution with the special spherical nanosized capsules **1a**, which leads also to a new type of supramolecular species.



The reaction of an aqueous solution of **1†** (obtainable in high yields in a facile synthesis; see experimental section) with hydrated Al³⁺ leads to the formation of the capsule anion **2a**. The corresponding compound **2†**, was characterised by elemental analyses, thermogravimetry (to determine the amount of water of crystallisation), redox titration (to determine the number of Mo^V centres), spectroscopic methods (IR, Raman, UV-VIS), as well as single-crystal X-ray structure analysis (including bond valence sum calculations).§



Compound **2** crystallises in the space group C2/c; it contains the anionic capsule **2a** with the “classical skeleton” of the above mentioned capsules, which is formed by 12 pentagonal units of

the type {(Mo^{VI})Mo^{VI}₅} positioned at the vertices of an icosahedron and connected by 30 {Mo^V₂O₄(SO₄)} linking groups. As a result of this construction principle the capsules contain 20

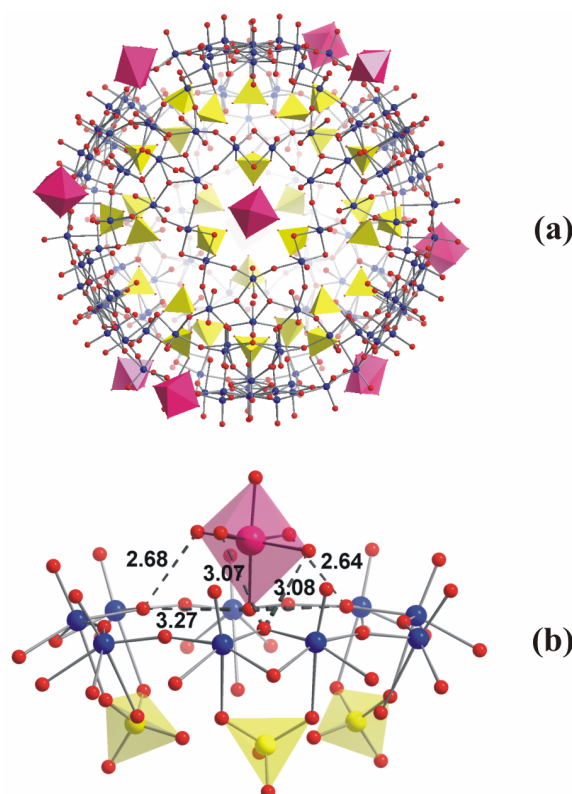


Fig. 1 (a) The structure of the anion **2a** mostly in ball-and-stick representation but highlighting the sulfate ligands (yellow tetrahedra) as well as the [Al(H₂O)₆]³⁺ complexes above the pores (pink octahedra); (b) the segment shows the type of {Mo₉O₉} pores – [Al(H₂O)₆]³⁺ interaction (with distances in Å); (colour code: Mo blue, O red).

pores, 20 channels, and a functionisable/modifiable cavity shell (see *e.g.* ref. 3).

According to the results of a single crystal X-ray structure analysis ten [Al(H₂O)₆]³⁺ complexes are positioned above the pores whilst the total number of the Al³⁺ cations in **2** is larger according to elemental analysis. The octahedral [Al(H₂O)₆]³⁺ complexes (Fig. 1a), are attracted by the negatively charged capsule and fixed through hydrogen bonds formed between their H₂O ligands and the O atoms of the capsule’s {Mo₉O₉} pores. The related Al-O-H…O distances are correspondingly in the range 2.6-3.2Å (Fig. 1b).⁴

* a.mueller@uni-bielefeld.de

After the removal of their hydration shell, many small cations are small enough to enter through the channels and getting finally positioned within the inner part of the capsule. But this is not possible in case of Al^{3+} cations (at least not completely), as the ligands of the $[\text{Al}(\text{H}_2\text{O})_6]^{3+}$ type complexes are rather strongly fixed.^{5,6} As a consequence of that we find $[\text{Al}(\text{H}_2\text{O})_6]^{3+}$ complexes fixed above the pores. An example for the opposite situation: as the larger Na^+ cations ($r_1 = 0.96 \text{ \AA}$ for Na^+ , $r_1 = 0.56 \text{ \AA}$ for Al^{3+} ⁷) form only weak aqua complexes, they can slip out their water coat, at least in part, cross the channel and recombine their ligand shell with oxygen donors that are available from the SO_4^{2-} ligands and from the encapsulated H_2O assemblies present in the cavity.³ In this context it is interesting to refer also to the bacterial K^+ channels which allows the passage of K^+ but not of the Na^+ ions which are too small for the channels to interact strongly with the channel CO-functions; whereas the environment of K^+ with O atoms does (approximately) not change after uptake so that the dehydration enthalpy is compensated. Based on that, it can be understood that the uptake of Na^+ is energetically not favoured.⁸

The present investigation proves the versatile applicability of the mentioned capsules e.g. the investigation of the strength of the interaction with metal aqua ions. In the special case of Al^{3+} different aqua ions are present in water depending upon their pH, while the most appropriate should be preferably trapped if it fits

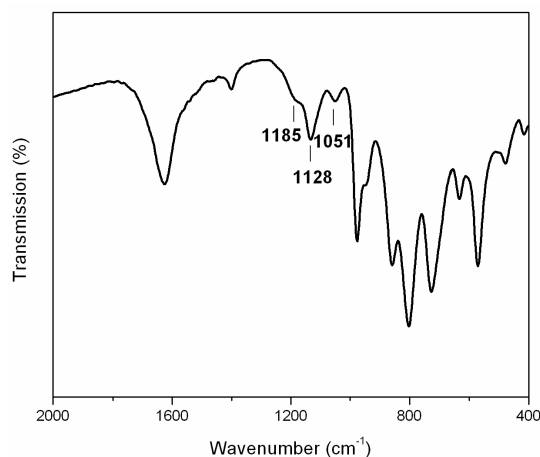


Fig. 2 IR-spectrum of **2** (KBr pellet) showing the wavenumbers of the $\nu_{\text{as}}(\text{SO}_4)$ triplet.

of course stereochemically with the pore geometry. The present result is mainly influenced by the slow H_2O ligand exchange (it can even be detected with ^{17}O NMR^{5a}). Correspondingly Al^{3+} has one of the highest hydration enthalpies for cations known (and even comparable with that of Ti^{3+} see ref. 5b).

On the other hand the incorporation of a few Al^{3+} cations can not be ruled out.‡ (The presence of uptaken Al^{3+} can of course not be proven by single crystal X-ray structure analysis because of the relevant disorder in connection with the abundance of a rather small number.) The coordination inside the cavity should be to the sulfate ligands (see ref. 9), which is to some extent supported by infrared spectroscopy (Fig. 2). Whereas the characteristic splitting of the triply degenerated $\nu_{\text{as}}(\text{SO}_4)$ mode is caused due to the bidentate coordination of the anion to the $\{\text{Mo}^{\text{V}}_2\text{O}_4\}^{2+}$ linkers, the position of the band at lowest wavenumbers of the triplet supports according to its monitor function Al^{3+} coordination (for arguments see ref. 9). The fact that well defined water cluster shells are not observed in **2a** in contrary to other sulfate type capsules,¹⁰ also supports the incorporation of

some Al^{3+} cations. The high charge density of the metal cations seems not to allow water shell formation.

Because of the relatively high concentration of Al^{3+} cations in the solution (50 times more Al^{3+} cations than NH_4^+ cations) and their high charge densities, there is the strong tendency of NH_4^+ versus Al^{3+} counter-transport related to a change from **1a** to **2a**. (Note: in spite of the strong $\text{H}_2\text{O}-\text{Al}^{3+}$ interaction, the high

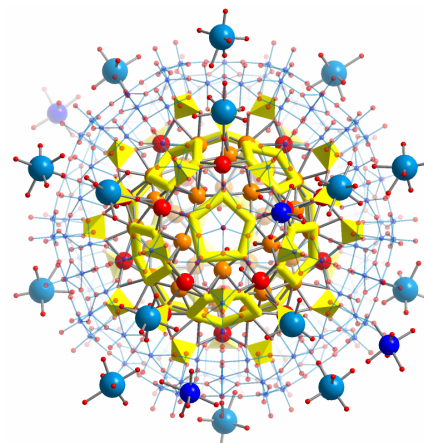


Fig. 3 Structure of an anion with surface environment obtained by the reaction of an aqueous solution of **1** with Mn^{2+} ions mostly in ball-and-stick representation. Mn^{2+} cations are found (1) inside the capsule disordered over two different types of positions: (a) disordered over 30 equivalent positions^{6c} (orange), while each underoccupied Mn^{2+} centre is coordinated in a bidentate fashion to only one SO_4^{2-} ligand (yellow polyhedra) and (b) disordered over 20 equivalent positions^{6c} (red) corresponding to sites at the C_3 -axes, in the centre of triangles spanned by three oxygen atoms of three different SO_4^{2-} ligands; and (2) in form of hydrated Mn^{2+} cations (a) above the pores (light blue) and (b) coordinated to a terminal O atom of the pentagonal units of the type $\{(\text{Mo}^{\text{VI}})\text{Mo}^{\text{VI}}_5\}$ of the metal framework (blue). The water cluster shells are - compared to other systems¹⁰ - distorted because of the encapsulated Mn^{2+} cations. (Fragments of the inner water shell are highlighted in yellow.¹¹)

charge of the cations supports uptake due to direct attractive interaction.) Though the present capsule skeleton, of course, cannot be directly compared with the cell membrane, it nevertheless allows modelling of some basic counter-transport ion phenomena.

The investigation of the capsule environment-interaction can be extended in a general way to the systematic study, to get information how easy water ligands can be released from cation environments. An instructive example refers to the different "behaviour" of the Ni^{2+} and Mn^{2+} (no crystal field stabilization) complexes in the sense that some Mn^{2+} get encapsulated (Fig. 3) but not the Ni^{2+} centres, where all get trapped with their six H_2O ligands above the pores. Structural details for the two cases will be published later.¹¹

The work opens up new perspectives for a special type of encapsulation chemistry,¹² i.e. coordination chemistry under confined conditions as well as on sphere surfaces.

The authors gratefully acknowledge the financial support of the Deutsche Forschungsgemeinschaft, the Fonds der Chemischen Industrie, the Volkswagenstiftung, the GIF and the European Union. A. Merca thanks the "Graduiertenkolleg Strukturbildungsprozesse", Universität Bielefeld, for a fellowship.

A. Müller,^{*a} A. Merca,^a H. Bögge,^a M. Schmidtman^a and A. Berkle^a

^a Fakultät für Chemie der Universität, Lehrstuhl für Anorganische Chemie I, Postfach 100131, D- 33501 Bielefeld, Germany. E-mail: a.mueller@uni-bielefeld.de

Notes and references

† *Synthesis of 1*: $(\text{NH}_4)_{42}[\text{Mo}_{132}\text{O}_{372}(\text{H}_2\text{O})_{72}(\text{CH}_3\text{COO})_{30}]$ ca. $(10\text{CH}_3\text{COONH}_4 + 300\text{H}_2\text{O})$ (2 g, 0.07 mmol) (See the ref. [2d] for the synthesis) is dissolved in 160 ml of water and $(\text{NH}_4)_2\text{SO}_4$ (8 g, 60.5 mmol) is added. The resulted solution is acidified with 21 ml 2M H_2SO_4 under stirring condition (pH \approx 1). After 2 weeks of crystallization in an open beaker brown crystals are filtered and washed with a small amount of 2-propanol. Yield: 1.8 g. Found: N, 3.5; S, 3.6 %. Calc.: N, 3.5; S 3.35 %. (This synthesis is easier than the earlier reported one in ref. 10a.)

Characteristic IR bands: ν/cm^{-1} (KBr pellet) 1618 (m, $\delta(\text{H}_2\text{O})$), 1404 (s, $\delta(\text{NH}_4)$), 1188 (m), 1136 (m), 1038(w-m), (all $\nu_{\text{as}}(\text{SO}_4)$), 970(s), 935(m) ($\nu(\text{Mo}=\text{O})$), 856(s), 800(vs), 727(s), 631(w-m), 571(m-s).

Characteristic Raman bands: ν/cm^{-1} (solid state, KBr dilution, $\lambda_{\text{e}} \sim 1064$ nm) 949 (m), 881 (s) ($\nu(\text{Mo}=\text{O})$), 374(m), 304 (w) cm^{-1} .

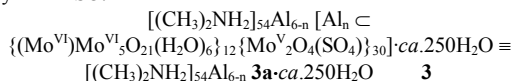
Synthesis of 2: To a solution of compound **1** (0.5 g, 0.017 mmol) in 30 ml H_2O in a 100 ml beaker, $\text{AlCl}_3 \cdot 6\text{H}_2\text{O}$ (5 g, 21 mmol) is added (pH \approx 2). The resulted solution was stirred for 1h and than was left for crystallization. After 10d dark brown crystals of **2** were filtered and washed with cold 2-propanol. Yield: 0.4g. Found: Al (gravimetrically), 1.6; N, 0.25 %. Calc.: Al, 1.6; N, 1 %.

Characteristic IR bands: ν/cm^{-1} (KBr pellet) 1629 (m, $\delta(\text{H}_2\text{O})$), 1404 (w-m, $\delta(\text{NH}_4)$), 1185 (w), 1128 (m-w), 1051 (w) (all $\nu_{\text{as}}(\text{SO}_4)$), 977(s), 948(m) ($\nu(\text{Mo}=\text{O})$), 858(s), 802(vs), 725(s), 630(m), 569(s), 478(m) cm^{-1} .

Characteristic Raman bands: ν/cm^{-1} (solid state, KBr dilution, $\lambda_{\text{e}} \sim 1064$ nm) 951 (w), 880 (s) ($\nu(\text{Mo}=\text{O})$), 479 (w), 430 (w), 375 (m), 304 (w-m) cm^{-1} .

§ *Crystal data for 2*: $\text{H}_{528}\text{Mo}_{132}\text{N}_{21}\text{O}_{714}\text{Al}_{17}\text{S}_{30}$, $M = 26334.65$ g mol⁻¹, monoclinic, space group $\text{C}2/c$, $a = 45.5106(21)$, $b = 46.3649(22)$, $c = 45.9510(21)$ Å, $\beta = 90.014$, $V = 96960(7)$ Å³, $Z = 4$, $\rho = 1.902$ g/cm³, $\mu = 1.83$ mm⁻¹, $F(000) = 53936$, crystal size = $0.30 \times 0.25 \times 0.20$ mm³. Crystals of **2** were removed from the mother liquor and immediately cooled to 188(2) K on a Bruker AXS SMART diffractometer (three circle goniometer with 1K CCD detector, Mo- K_{α} radiation, graphite monochromator; hemisphere data collection in ω at 0.3° scan width in three runs with 606, 435 and 230 frames ($\Phi = 0, 88$ and 180°) at a detector distance of 5.00 cm). A total of 290395 reflections ($1.53 < \theta < 26.99^\circ$) were collected of which 105063 reflections were unique ($R(\text{int}) = 0.0466$). An empirical absorption correction using equivalent reflections was performed with the program SADABS. The structure was solved with the program SHELXS-97 and refined using SHELXL-97 to $R = 0.0666$ for 74538 reflections with $I > 2\sigma(I)$, $R = 0.1084$ for all reflections; max./min. residual electron density 1.71 and -1.15 e Å⁻³ SHELXS/L, SADABS from G.M. Sheldrick, University of Göttingen, 1993/97; structure graphics with DIAMOND 2.1 from K. Brandenburg, Crystal Impact GbR, 2001).

‡ Because **2** is insoluble in water or organic solvents (DMSO, DMF), solution based investigations could not be made; therefore we reacted an aqueous solution of **1** with Al^{3+} in the presence of $[(\text{CH}_3)_2\text{NH}_2]^+$ cations which leads to the formation of compound **3**, which is soluble in H_2O and partially in DMSO.



The formula of **3** was established by elemental analysis and spectroscopic methods (IR, Raman, UV-VIS). In case of **3a** the Al^{3+} cations can not be located by single crystal X-ray structure analysis because of the high disorder. The knowledge of compound **3** will allow later solutions studies which can prove the encapsulation of the Al^{3+} cations by ²⁷Al-NMR studies.

Elemental Analysis: Found: Al (gravimetrically), 0.42; C, 3.7; N, 2.1 %. Calc.: Al, 0.51; C, 4.2; N, 2.4 %.

Characteristic IR bands: ν/cm^{-1} (KBr pellet) 1624 (m, $\delta(\text{H}_2\text{O})$), 1461 (w-m, $\delta(\text{NH}_4)$), 1404 (w), 1180 (w), 1130 (m-w), 1045 (w) (all $\nu_{\text{as}}(\text{SO}_4)$), 1022 (w, $\nu(\text{CN})$) 972(s), 948(m) (s, $\nu(\text{Mo}=\text{O})$), 860(s), 802(vs), 729(s), 633(m), 570(s), 474(m) cm^{-1} .

Characteristic Raman bands: ν/cm^{-1} (solid state, KBr dilution, $\lambda_{\text{e}} \sim 1064$ nm) 951 (w), 880 (s) ($\nu(\text{Mo}=\text{O})$), 479 (w), 430 (w), 375 (m), 304 (w-m) cm^{-1} .

1. E. L. Wolf, *Nanophysics and Nanotechnology, An Introduction to Modern Concepts in Nanoscience*, Wiley-VCH, Weinheim, 2004.
2. (a) A. Müller, P. Kögerler, C. Kuhlmann, *Chem. Commun.*, 1999, 1347; (b) A. Müller, S. Roy, *Coord. Chem. Rev.*, 2003, **245**, 153; (c) L. Cronin, E. Diemann, A. Müller in *Inorganic Experiments* (Ed.: D. Woollins), Wiley-VCH, Weinheim, 2003, p.340; (d) A. Müller, S. K. Das, E. Krickemeyer, C. Kuhlmann, *Inorg. Synth.*, 2004, **34** (Ed.: J. Shapley), p.191; (e) L. Cronin in *Comprehensive Coordination Chemistry II* (Eds.: J. A McCleverty, T. J. Meyer), Vol. 7, p.1- 57, Amsterdam, Elsevier, 2004.
3. A. Müller, S. K. Das, S. Talismanov, S. Roy, E. Beckmann, H. Bögge, M. Schmidtman, A. Merca, A. Berkle, L. Allouche, Y. Zhou, L. Zhang, *Angew. Chem. Int. Ed.*, 2003, **42**, 5039.
4. An investigation of the Al^{3+} uptake was also performed at varying pH values (pH range from 1 to 2.5) interestingly without observation of any significant changes.
5. (a) D. T. Richens, *The Chemistry of Aqua Ions*, Wiley, Chichester, 1997; (b) F. A. Cotton, G. Wilkinson, C. A. Murillo and M. Bochmann, *Advanced Inorganic Chemistry*, 6th edn., Wiley-VCH, New York, 1999, p.58 and p.183; (c) A.E. Martell, R.D. Hancock, *Metal Complexes in Aqueous Solutions*, Plenum Press, New York, 1996.
6. (a) H. Krüger, *Chem. Soc. Revs.*, 1982, **11**, 227; (b) G. W. Neilson and J. E. Enderby, *Adv. Inorg. Chem.*, 1989, **34**, 195; (c) A. Müller, H. Bögge and M. Henry, *C. R. Chimie*, 2005, **8**, 47.
7. Y. Marcus, H. D. B. Jenkins, L. Glasser, *J. Chem. Soc., Dalton Trans.*, 2002, 3795.
8. R. MacKinnon, *Angew. Chem. Int. Ed.*, 2004, **43**, 4265, and ref. therein.
9. A. Müller, D. Rehder, E. T. K. Haupt, A. Merca, H. Bögge, M. Schmidtman, G. Heinze-Brückner, *Angew. Chem. Int. Ed.*, 2004, **43**, 4466; Corrigendum: **43**, 5115.
10. (a) A. Müller, E. Krickemeyer, H. Bögge, M. Schmidtman, B. Botar, M. O. Talismanova, *Angew. Chem. Int. Ed.*, 2003, **42**, 2085; (b) A. Müller, E. Krickemeyer, H. Bögge, M. Schmidtman, S. Roy, A. Berkle, *Angew. Chem. Int. Ed.*, 2002, **41**, 3509; (c) M. Henry, H. Bögge, E. Diemann, A. Müller, *J. Mol. Liquids*, 2005, **118**, 155; (d) A. Müller, H. Bögge, E. Diemann, *Inorg. Chem. Comm.*, 2003, **6**, 52.
11. A. Müller, Y. Zhou, H. Bögge, M. Schmidtman, L. Zhang to be published.
12. (a) M. Gross, *Chem. Br.*, 2003, **39**(8), 18; (b) W. G. Klemperer and G. Westwood, *Nat. Mater.*, 2003, **2**, 780.

Artificial Cells: Temperature-Dependent, Reversible Li⁺-Ion Uptake/Release Equilibrium at Metal Oxide Nanocontainer Pores**

Achim Müller,* Dieter Rehder,* Erhard T. K. Haupt, Alice Merca, Hartmut Bögge, Marc Schmidtman, and Gabriele Heinze-Brückner

Dedicated to Professor Martin Jansen
on the occasion of his 60th birthday

Whereas a large number of porous materials exist as extended structures, as yet very little is known about well-defined, discrete, stable, and soluble (molecular) nanoporous capsules. These capsules allow the systematic study of processes in solution related to the uptake/release of substrates such as cations, with the possibility of extending such studies to related cation–cation countertransport processes. The prediction of the affinity of *specific* substrates for *specific* areas of the capsule is of particular interest as insight may be gained into a new type of chemistry that could be performed under confined conditions.

This is the case for spherical nanosized capsules based on the rather robust fundamental skeleton (pent)₁₂(linker)₃₀ ≡ {(Mo^{VI})Mo₅^{VI}O₂₁(H₂O)₆}₁₂{Mo₂^VO₄(ligand)}₃₀, such as in **1**,^[1] which is often employed as the starting material for other related compounds as it is easily prepared.^[2] The capsules have sizeable pores and finely sculptured interiors inbetween which lie functionalized channels that display unprecedented molecular-scale filter properties.^[3a] The size and charge of the capsules can be varied (Figure 1), whereas their affinity for (special) cations depends not only on the charge but also on the nature of the functional groups present inside the cavities.^[3b] This allows the transfer of ions in a controlled and specific fashion, reminiscent of the processes that already occur in Nature on a cellular level. With respect to cation-uptake processes and the competitive uptake/release of different cations (countertransport processes), the capsules

[*] Prof. Dr. A. Müller, A. Merca, Dr. H. Bögge, M. Schmidtman, G. Heinze-Brückner
Lehrstuhl für Anorganische Chemie I
Fakultät für Chemie der Universität
Postfach 100131, 33501 Bielefeld (Germany)
Fax: (+49) 521-106-6003
E-mail: a.mueller@uni-bielefeld.de
Prof. Dr. D. Rehder, Dr. E. T. K. Haupt
Institut für Anorganische und Angewandte Chemie
der Universität Hamburg
Martin-Luther-King-Platz 6, 20146 Hamburg (Germany)
Fax: (+49) 40-42838-2893
E-mail: dieter.rehder@chemie.uni-hamburg.de

[**] The authors gratefully acknowledge the financial support of the Deutsche Forschungsgemeinschaft, the Fonds der Chemischen Industrie, the Volkswagenstiftung, and the European Union (HPRN-CT-1999-00012). A. Merca thanks the "Graduiertenkolleg Struktur-bildungsprozesse", Universität Bielefeld, for a fellowship.

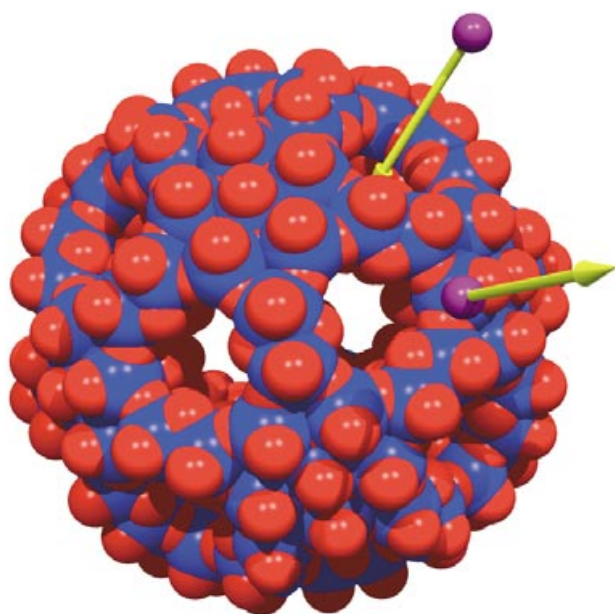
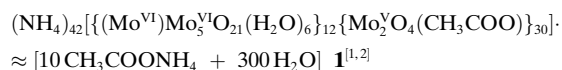


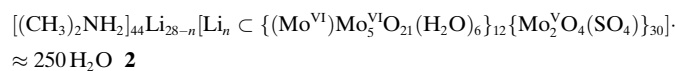
Figure 1. Schematic space-filling representation of the uptake and release of cations such as Li^+ through some of the 20 pores of highly charged anionic capsules of the structure type **2a** (Mo blue, O red).

can be considered formally as artificial cells in as much as they exhibit ion channels^[3b,c] and may allow chemistry to be performed on the nanoscale in the future.^[3d]



Herein, we report the stability and the use/applicability of this type of capsule in solution (details about the relative stabilities of capsules with different ligands in different solvents will be published later). A temperature-dependent equilibrium process that involves the uptake/release of Li^+ ions through the capsule pores and channels is also shown to be present. The results bear some relation as a model for Li^+ ion transport processes in clinical chemistry research.

The uptake/release of Li^+ ions was studied by ^7Li NMR spectroscopic analysis of solutions of compound **2**, which comprises the capsule skeleton mentioned earlier. Treatment of an aqueous solution of **1** with Li_2SO_4 in the presence of $[(\text{CH}_3)_2\text{NH}_2]^+$ cations (to render the compound soluble in DMSO) led to the formation of compound **2**, which was characterized by elemental analysis, thermogravimetry (to determine the amount of water of crystallization), flame photometry (to determine the number of Li^+ cations), redox titrations (to determine the number of Mo^{V} centers), spectroscopy (IR, Raman, UV/Vis), as well as X-ray single-crystal structure analysis^[4] (including bond valence sum calculations), and ^7Li NMR spectroscopy.^[5]



Compound **2** crystallizes in the space group $R\bar{3}$ and is soluble in H_2O and DMSO. Its anionic capsule **2a** contains

20 pores, 20 channels, and a functionalized cavity (see also reference [3a]). The incorporation of Li^+ cations can easily be detected by IR^[6a] and especially ^7Li NMR spectroscopy, but is only indirectly detected by X-ray single-crystal structure analysis. Figure 2 shows sections of the crystal structure of **2a**

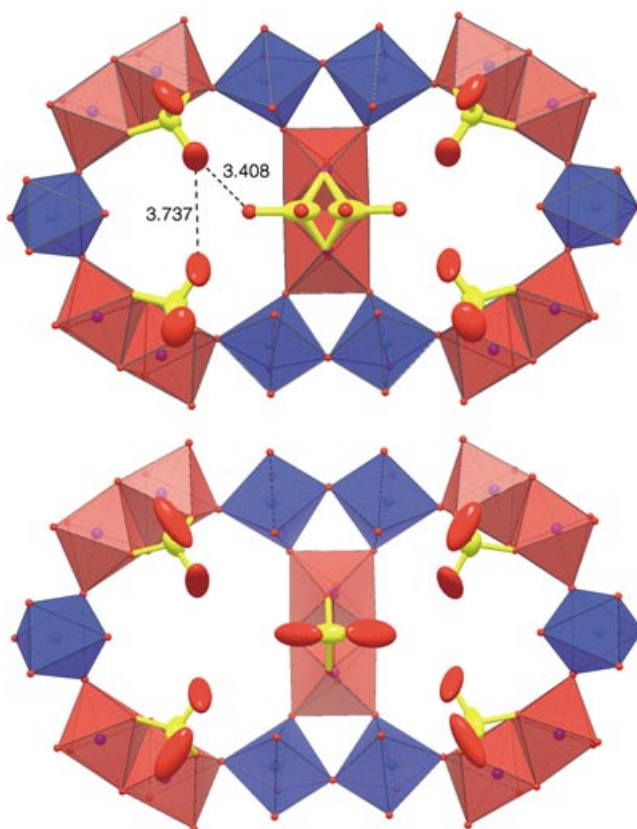


Figure 2. Outline of two of the 20 pores, as well as below-pore sections, of the anions **2a** (bottom) and the related anion **3a** (top).^[4] Whereas in the case of **2a**, the disorder could not be resolved for the SO_4^{2-} ligands—although the size and shape of their thermal ellipsoids clearly reflect the influence of Li^+ (bottom)—the disorder was successfully resolved for a sulfate ligand of **3a** (top). Shown are: 1) the MoO_6 polyhedra (binuclear linkers in red) that form two adjacent pores— Mo_9O_9 rings with an average ring-aperture of ≈ 0.45 nm (for example, see reference [3a]), and 2) the SO_4^{2-} ligands coordinated to the $\{\text{Mo}_2\}$ linkers below the pores. The disorder for the SO_4^{2-} ligand coordinated to the “central” $\{\text{Mo}_2\}$ group is caused by “directly non-observable” Li^+ cations, giving rise to the respective distances (top).

and of the related structure **3a**, which is abundant in the compound $\text{Li}_{65}(\text{NH}_4)_7[\{(\text{Mo}^{\text{VI}})\text{Mo}_5^{\text{VI}}\text{O}_{21}(\text{H}_2\text{O})_6\}_{12}\{\text{Mo}_2^{\text{V}}\text{O}_4(\text{SO}_4)\}_{30}] \cdot \approx 200 \text{H}_2\text{O}$ **3** $\equiv \text{Li}_{65}(\text{NH}_4)_7 \cdot \mathbf{3a} \cdot \approx 200 \text{H}_2\text{O}$; this material^[4] has a higher concentration of Li^+ ions^[5] but could not be considered in this case for NMR spectroscopic investigations as it is insoluble in DMSO.

From the present X-ray diffraction study (Figure 2), it is seen that the $\text{O}\cdots\text{O}$ distances between the three SO_4^{2-} ligands are too large (> 3.7 Å) for a symmetrical coordination of the Li^+ ion to all of the sulfate groups. Consequently, unsymmetrical coordination below the pore channels occurs (Figure 2, top). This is in contrast to the situation encountered with the larger Na^+ cations, which are symmetrically coordi-

nated to each of the three sulfate groups and which leads to a highly symmetrical $60 = 20 \times 3$ water “cluster” coordinated to the Na^+ cations.^[6b] Clearly, this is not possible in the present (unsymmetrical) case with Li^+ ions.

According to the Raman spectra, the capsules with icosahedral symmetry are quite stable in O_2 free solutions in H_2O and DMSO up to $\approx 60^\circ\text{C}$ (Figure 3). As the spectrum

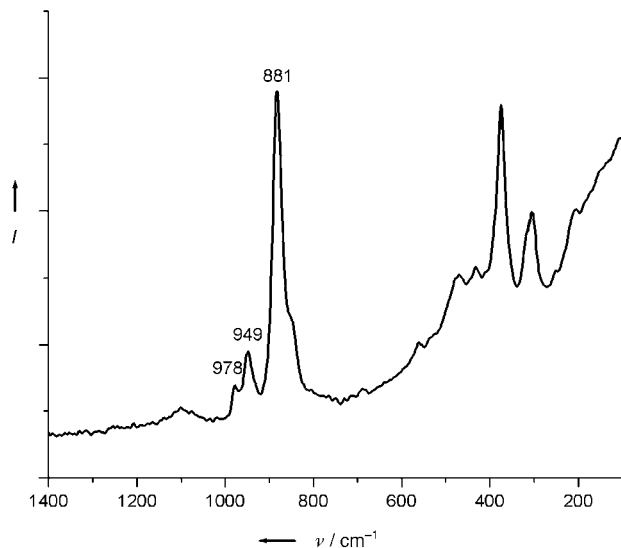


Figure 3. Raman spectrum of **2** in H_2O ($\lambda_{\text{exc}} = 1064 \text{ nm}$), which is practically identical to that of solid **2** and thus supports the reasonable stability of the highly symmetrical capsule **2a** in solution. The most intense band at 881 cm^{-1} corresponds to the totally symmetric A_g breathing vibrations of the capsule which involve predominantly 60 $\mu_3\text{-O}(\text{Mo}_3)$ surface atoms.

consists of only a few lines (note the possible fivefold degeneracy expected for the I_h point group, and that only A_g and H_g type vibrations are Raman allowed) this allows the easy detection of eventual decomposition even for such an extremely large molecular system. The bands are characteristic for the highly symmetrical molybdenum oxide based $\{(\text{Mo}^{\text{VI}})\text{Mo}_5^{\text{VI}}\}_{12}[\text{Mo}_2^{\text{V}}]_{30}$ type skeleton.

The ^7Li NMR spectrum^[7] of **2** dissolved in DMSO/ $[\text{D}_6]\text{DMSO}$ (1:1; $c(\text{Li}^+) \approx 50 \text{ mM}$; Figure 4) measured at room temperature shows two sharp signals at $\delta = -0.78$ and -0.80 ppm (I), which correspond to $[\text{Li}(\text{dms})_n]^+$ in the bulk solution (the peaks are identical to those in the spectrum of Li^+ ions in pure DMSO), and at least three broad (half-width ($W_{1/2}$) $\approx 80 \text{ Hz}$) overlapping signals centered at $\delta = -1.67$, -2.18 , and -2.56 ppm (II–IV; overall relative intensity $\approx 15\%$). These latter peaks are assigned to three different Li^+ -ion sites associated with the cluster $\text{Li}^+ \subset \mathbf{2a}$. The upfield shifts—with respect to $[\text{Li}(\text{dms})_n]^+$, $\delta \approx -0.79 \text{ ppm}$ —reflect the increased complexation of the Li^+ cations to negatively charged ligands such as sulfate, and/or bridging oxo groups such as at the Mo_6O_9 type rings/pores.^[8a] This pattern, which is observed immediately after the dissolution of **2**, does not change within several days; that is, the system readily reaches equilibrium and remains rather stable over an extended period of time. Furthermore, the temperature dependence of

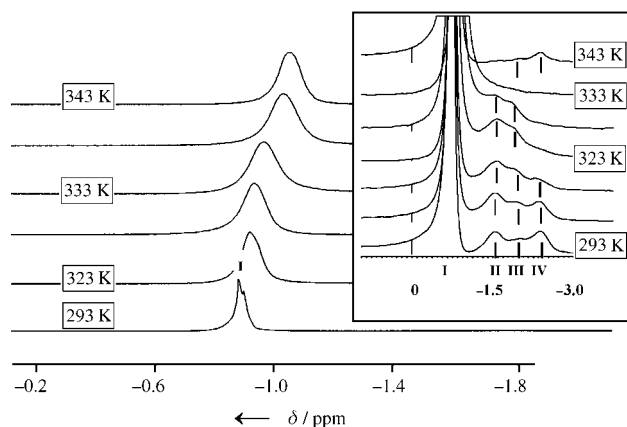
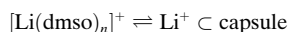


Figure 4. Variable-temperature ^7Li NMR spectra of **2** ($c(\mathbf{2}) \approx 1.8 \text{ mM}$) in DMSO/ $[\text{D}_6]\text{DMSO}$ 1:1. The inset shows the vertical expansion with the uppermost spectrum obtained after cooling back to room temperature. I ($\delta = -0.79 \text{ ppm}$) corresponds to $[\text{Li}(\text{dms})_n]^+$, whereas II ($\delta = -1.67 \text{ ppm}$), III ($\delta = -2.18 \text{ ppm}$), and IV ($\delta = -2.56 \text{ ppm}$) correspond to Li^+ sites associated with $\text{Li}^+ \subset \mathbf{2a}$.

the spectral patterns (Figure 4) with respect to both the broadening as well as the shifts (upfield for I, downfield for II, III, and IV) of the bands upon increasing the temperature, clearly indicates an exchange equilibrium between exterior and interior Li^+ ions.^[8b] The signal at $\delta = -2.56 \text{ ppm}$ (IV) disappears at about 330 K, whereas a complete coalescence of the signals for the system (signals I, II, III, and IV) occurs at 343 K (average $\delta = -0.96 \text{ ppm}$) representing very fast exchange within the equilibrium:

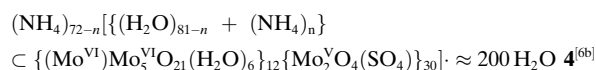


In the temperature range 293–343 K, the exchange process is largely reversible for two of the sites; upon cooling, the signals at $\delta = -2.18$ (III) and -2.56 ppm (IV) are almost restored. However, the signal at $\delta = -1.67 \text{ ppm}$ (II) does not reappear which suggests that one of the Li^+ -ion sites is not occupied again. The first of the upfield signals, II, is assigned to Li^+ ions coordinated to the sulfate group which was also proven from crystallographic studies and IR spectroscopic measurements. This site is the furthest distance away from the pore area/cluster periphery and is correspondingly not reoccupied after cooling as the sites closer to the capsule periphery (peaks III and IV) are the first to be reoccupied, which decreases the affinity of the capsule for cations. The more-peripheral sites have a higher electron density (in agreement with a classical Pauling rule) with the consequence that the related peaks are found at higher fields.

Complementary to the temperature-dependent behavior of the signals, the $[\text{Li}(\text{dms})_n]^+ - \text{Li}^+(\text{capsule})$ -exchange process has been confirmed by ^7Li - ^2D exchange spectroscopy (EXSY) of solutions of **2** in DMSO ($c(\mathbf{2}) = 1 \text{ mM}$; $c(\text{Li}^+) = 30 \text{ mM}$; slow exchange conditions at room temperature and a mixing time of 1.5 s were employed). The EXSY spectrum (not shown here) displays cross-peaks owing to a magnetization transfer between external (signal I) and internal Li^+ ions (signals II–IV) which disappear upon the addition of an

excess of guanidinium chloride ($c = 30$ mM); guanidinium cations prevent exchange through blockage of the capsule pores (see reference [6c]). Concomitantly, signals II and III almost disappear and a new signal representing 5% of the overall integral intensity appears at $\delta = -3.1$ ppm.

Treatment of a solution of **4** in DMSO with a 20-fold molar excess of LiCl leads to the uptake/incorporation of about 12% of the Li⁺ ions as observed from a broad signal at $\delta = -2.03$ ppm for Li⁺ in **4a**. This signal is accompanied by the resonance for [Li(dmsO)_n]⁺ at $\delta = -0.82$ ppm with an upfield shoulder at about $\delta = -1.05$ ppm. The situation is comparable to the system Li⁺ in **2a** in as far as the Li⁺ ions are apparently taken up by the cluster under changed conditions. In the case of the anionic capsule **4a**, for example, Li⁺ competes with NH₄⁺ to some extent for the capsule sites.



The present study of the uptake/release of cations by a capsule in solution may be extended to investigate nanoscale reactions in solutions (see also reference [3d]) as well as a large variety of cation-transport phenomena (e.g. competition processes) in different solvents^[9]; furthermore, unique hydration structures can be investigated under restricted conditions. An important aspect is that the interiors, sizes, and pores of the capsules can be varied to allow different cation-affinity properties. Interestingly, the transport of cations under physiological conditions (e.g. Li⁺-ion transmembrane transport and storage) can, in principle, be modeled. Also, there is the possibility to model important transport pathways of medicinal interest, such as the Li⁺-Na⁺ countertransport process (of interest in hypertension research) in which Na⁺ ions enter and Li⁺ ions leave erythrocytes in order to maintain the Na⁺ ion balance in the cells and the plasma.^[10–12]

Experimental Section

2: The pH value of a solution of **1** (2.0 g, 0.068 mmol) and Li₂SO₄·H₂O (10 g, 78 mmol) in H₂O (80 mL) was adjusted to ≈ 2.2 with aqueous H₂SO₄ (0.5 M), and the solution was stirred for 5 h at room temperature. (The large excess of Li₂SO₄ was necessary first, owing to the large number of functional groups present in the capsule, e.g. 30 SO₄²⁻ groups and 180 Mo₃O₉ type O atoms, and second, to isolate the highly water soluble product **2** as a salt, and third, because of the high affinity of Li⁺ to water.) The temperature of the solution was increased to 70 °C over 30 min, then (CH₃)₂NH₂Cl (1.5 g, 18.39 mmol) was added, and the solution was stirred at this temperature for a further 30 min. The hot solution was filtered, then the cooled dark brown filtrate was stored at 20 °C to effect crystallization. After 4 days, the precipitated dark brown, parallelepiped crystals of **2** were isolated by filtration and dried in air (70% based on **1**); elemental analysis: calcd for C₈₈H₉₉₆Li₂₈Mo₁₃₂N₄₄O₈₁₄S₃₀: C 3.58, N 2.08, Li 0.65; found: C 3.6, N 2.1, Li (flame photometry) 0.6; IR (KBr): $\tilde{\nu} = 1622$ (m, $\delta(\text{H}_2\text{O})$), 1463 (w-m, $\delta_{\text{as}}(\text{CH}_3)$), 1183 (w), 1137 (m-w), 1053 (w, $\nu_{\text{as}}(\text{SO}_4)$ triplet), 975 (s), 943 (m, $\nu(\text{Mo}=\text{O})$), 860 (s), 802 (vs), 729 (s), 634 (m), 574 cm⁻¹ (s); FT-Raman (see Figure 3); UV/Vis (H₂O): $\lambda = 459$ nm.

Received: January 15, 2004

Revised: May 19, 2004 [Z53762]

Keywords: artificial cells · ion channels · lithium · nanostructures · porous materials

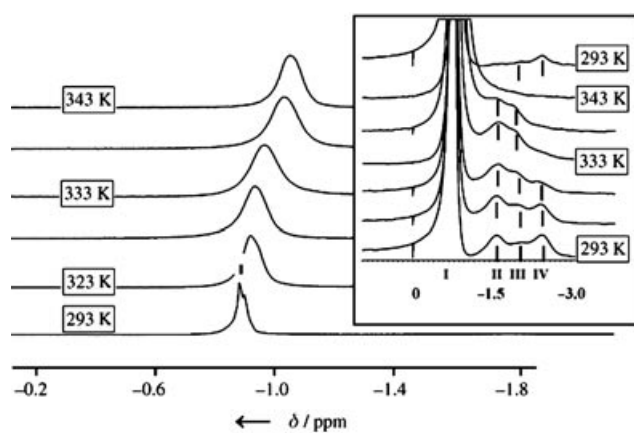
- [1] For a review, see: A. Müller, P. Kögerler, C. Kuhlmann, *Chem. Commun.* **1999**, 1347–1358.
- [2] a) A. Müller, S. K. Das, E. Krickemeyer, C. Kuhlmann, *Inorg. Synth.* **2004**, *34*, 191–200; b) L. Cronin, E. Diemann, A. Müller in *Inorganic Experiments* (Ed.: J. D. Woollins), Wiley-VCH, Weinheim, **2003**, pp. 340–346.
- [3] a) A. Müller, S. K. Das, S. Talismanov, S. Roy, E. Beckmann, H. Bögge, M. Schmidtman, A. Merca, A. Berkle, L. Allouche, Y. Zhou, L. Zhang, *Angew. Chem.* **2003**, *115*, 5193–5198; *Angew. Chem. Int. Ed.* **2003**, *42*, 5039–5044; in all the cases studied therein, the positioning of the cations was clearly understood except for that of Rb⁺—this was attributed to the influence of the crystallization process, which does not influence the results in the present solution process. b) An extreme affinity is observed for the sulfate type capsule in the case of Ca²⁺ as 20 of these ions can be positioned at the end of the 20 channels at specific positions where also Na⁺ cations, although in a smaller amount, can be positioned^[3a]—in doing so, the entrance to the central cavity is completely blocked (unpublished results). In cases where the encapsulated cation positions cannot be determined, the given charge refers to that of the empty capsule^[1,2] (see also **3**). c) Interesting cation uptake (and also the uptake of anions and water molecules) under confined conditions has also been observed for nanotube structures, but such a situation does not easily allow an equilibrium study to be performed in solution; see: T. Ohkubo, Y. Hattori, H. Kanoh, T. Konishi, T. Fujikawa, K. Kaneko, *J. Phys. Chem. B* **2003**, *107*, 13616–13622; T. Ohkubo, H. Kanoh, K. Kaneko, *Aust. J. Chem.* **2003**, *56*, 1013–1016; see also: d) “Traps for cations”: W. G. Klemperer, G. Westwood, *Nat. Mater.* **2004**, *2*, 780–781.
- [4] Crystal data for **2** (C₈₈H₉₉₆Li₂₈Mo₁₃₂N₄₄O₈₁₄S₃₀): $M = 29521.49$ g mol⁻¹, rhombohedral, space group $R\bar{3}$, $a = 32.8188(12)$, $c = 74.350(4)$ Å, $V = 69352(5)$ Å³, $Z = 3$, $\rho = 2.121$ g cm⁻³, $\mu = 1.908$ mm⁻¹, $F(000) = 43356$, crystal size = $0.30 \times 0.25 \times 0.20$ mm³; crystals of **2** were removed from the mother liquor and immediately cooled to 188(2) K on a Bruker AXS SMART diffractometer (three cycle goniometer with 1 K CCD detector, Mo_{K α} radiation, graphite monochromator; hemisphere data collection in ω at 0.3° scan width in three runs with 606, 435, and 230 frames ($\phi = 0, 88, \text{ and } 180^\circ$) at a detector distance of 5.0 cm). A total of 135812 reflections ($1.53 < \theta < 26.99^\circ$) were collected of which 33506 reflections were unique ($R_{\text{int}} = 0.0429$). An empirical absorption correction using equivalent reflections was performed with the program SADABS. The structure was solved with the program SHELXS-97 and refined with SHELXL-97 to $R = 0.0506$ for 25064 reflections with $I > 2\sigma(I)$, $R = 0.0763$ for all reflections; max./min. residual electron density 1.613 and -1.785 e Å⁻³ (SHELXS/L, SADABS from G. M. Sheldrick, University of Göttingen 1997/2001; structure graphics with DIAMOND 2.1 from K. Brandenburg, Crystal Impact GbR, 2001). CCDC 228367 contains the supplementary crystallographic data for this paper. These data can be obtained free of charge via www.ccdc.cam.ac.uk/conts/retrieving.html (or from the Cambridge Crystallographic Data Centre, 12, Union Road, Cambridge CB21EZ, UK; fax: (+44) 1223-336-033; or deposit@ccdc.cam.ac.uk). Cell parameters for **3**: monoclinic space group $C2/m$, $a = 44.483(2)$, $b = 40.077(2)$, $c = 31.757(2)$ Å, $\beta = 134.116(1)^\circ$, $V = 40645(5)$ Å³.
- [5] ⁷Li NMR spectra of solutions were recorded on a Bruker Avance 400 spectrometer (155.51 MHz) in rotating 10-mm diameter tubes; acquisition time 2.1 s, relaxation delay 2 s, pulse width 30°. All data are reported relative to the reference material (9.7 M LiCl in D₂O, according to: R. K. Harris, E. D.

Becker, S. M. Cabral de Menezes, R. Goodfellow, P. Granger, *Pure Appl. Chem.* **2001**, *73*, 1795–1818). Area calibration was carried out by insertion of a coaxial inset containing LiCl (0.1M in $[D_6]DMF$, $\delta = +0.90$). The Lorentzian line-shape analysis was performed for four lines by using the ‘deconvolution 1’ feature of the Bruker WINNMR V6.0 program.

- [6] a) Compound **2** shows a triplet 1183/1137/1053 cm^{-1} in the IR spectrum which originates from the bidentate coordination of the sulfate anion (ν_{as} mode of the “free” SO_4^{2-} ion lies at ca. 1105 cm^{-1}); see: K. Nakamoto, *Infrared and Raman Spectra of Inorganic and Coordination Compounds*, 5th ed., Wiley, New York, **1997**, Part A, p. 199; Part B, pp. 79–82. As the SO_4^{2-} groups are located *trans* to the Mo=O bonds the coordination is rather weak, with the consequence that the “terminal” sulfate O atoms show a higher electron density than in the case of a stronger ligand coordination. This can strengthen (relatively) the interaction with encapsulated cations, being again stronger for Li^+ ions than in general for Na^+/NH_4^+ ions (note that one Na^+ ion is coordinated to three sulfate ligands in the capsule, whereas Li^+ is predominantly coordinated to one SO_4^{2-} group and so the interaction per sulfate ligand is therefore larger).^[6b] In the case of related Na^+/NH_4^+ salts, the two bands at higher energy are observed at nearly the same wavenumbers as the corresponding bands for **2a**, whereas the lower energy band of the triplet occurs at $\approx 1040\text{ cm}^{-1}$ in the Na^+/NH_4^+ salts but at 1053 cm^{-1} in the case of **2a**. The same situation as in the case of the Na^+ and NH_4^+ capsules is found for a compound containing only guanidinium cations, which cannot enter the cavity;^[6c] this band consequently is also observed at 1038 cm^{-1} . (The assignment of the respective band for the guanidinium compound was rather difficult as it partially overlaps with the $O_2PH_2^-$ -bands).^[6c] The shift of the band in the case of **2a** is influenced by the rather strong interaction with Li^+ ions which partially decreases the negative charge on the sulfate and therefore strengthens the S–O bonds; b) A. Müller, E. Krickemeyer, H. Bögge, M. Schmidtman, B. Botar, M. O. Talismanova, *Angew. Chem.* **2003**, *115*, 2131–2136; *Angew. Chem. Int. Ed.* **2003**, *42*, 2085–2090; the compound **4** can be obtained more easily and methodically (without the need for heating) by acidification of the solution to protonate the acetate ligands and render them better leaving groups; c) A. Müller, E. Krickemeyer, H. Bögge, M. Schmidtman, S. Roy, A. Berkle, *Angew. Chem.* **2002**, *114*, 3756–3761; *Angew. Chem. Int. Ed.* **2002**, *41*, 3604–3609.
- [7] a) J. W. Akitt in *Multinuclear NMR* (Ed.: J. Mason), Plenum, New York, **1987**, chap. 7; b) C. Detellier in *NMR of Newly Accessible Nuclei, Vol. 2* (Ed.: P. Laszlo), Academic Press, New York, **1983**, chap. 5; c) B. Lindmann, S. Forsén in *NMR and the Periodic Table* (Eds.: R. K. Harris, B. E. Mann), Academic Press, New York, **1978**, chap. 6.
- [8] a) The notation “increased complexation of Li^+ ” refers to the dominance of the paramagnetic contribution related to variations in shielding. In other words, paramagnetic shielding is expected to decrease (and overall shielding to increase) with the increasing expansion of the “electron cloud” around Li , to result in an increased covalency of the Li^+ –donor interaction as the contact between the Li^+ ion and the donor groups becomes more intimate. The signal IV could be attributed to the complexation of Li^+ ions by the oxo functions of the Mo_9O_9 ring, as this peak disappears the most easily, both upon heating and upon the addition of Na^+ ions. For the crown ether complex $[Li(15C5)]^+$, which may be compared to the coordination of Li^+ ions in the present study, a chemical shift value of $\delta = -1.8$ ppm was noted; see: A. I. Popov, *Pure Appl. Chem.* **1979**, *51*, 101. Importantly, the Mo^V centers in the binuclear unit are spin-coupled upon formation of a metal–metal bond, thereby excluding influences by paramagnetic centers; b) for an independent resonance signal, deshielding is expected upon an increase in the temperature as a consequence of the increased paramagnetic-deshielding contributions as the vibronic levels of the ground and excited states become more populated. Concomitantly, if the nucleus is quadrupolar as in the case of 7Li , the resonance should sharpen upon a decrease in the molecular correlation time (decreasing viscosity). In the present case, an increase in the shielding and broadening of the line widths is observed for signal I as the temperature is raised; the spectral patterns clearly indicate an exchange between exterior (I) and interior Li^+ ions (II, III, and IV).
- [9] For **2** dissolved in H_2O/D_2O , only one narrow 7Li resonance at $\delta = -0.16$ ppm ($W_{1/2} = 2.3$ Hz) is observed, which corresponds to hydrated Li^+ ions and is indicative of the complete extrusion of Li^+ ions into the aqueous medium. This arises from the higher affinity of Li^+ for water than for the functional capsule sites. Competitive-phenomena studies (e.g. Li^+/Na^+) performed in aqueous media in the presence of electrolytes (to reduce the affinity of the cations for the solvent, and to approximate physiological conditions) are currently underway. As far as the dielectric properties of the medium are concerned, serum and cytosol more closely resemble DMSO than water. Note that more than ten billion proteins are abundant in an animal cell and influence the properties of the water solvent.
- [10] Na^+ – Li^+ countertransport is an ion-transport process that exchanges sodium ions for lithium ions or other univalent cations. It was brought to clinical attention by Canessa et al., who reported that its activity was enhanced in the erythrocytes of patients with essential hypertension—a finding that was confirmed in many epidemiological and clinical studies thereafter; see: M. Canessa, N. Adragna, H. S. Solomon, T. M. Conolly, D. C. Tosteson, *New Engl. J. Med.* **1980**, *302*, 772–776; P. Strazzullo, A. Siani, F. P. Cappuccio, M. Trevisan, E. Ragona, L. Russo, R. Iacone, E. Farinara, *Hypertension* **1998**, *31*, 1284–1289. Although the capsule wall of our structure cannot be compared with the red-cell membrane, which perfectly balances the concentrations of cations and water so that the cells do not shrink, nevertheless, it allows fundamental countertransport phenomena to be measured; see: Y. Yawata, *Cell Membrane: The Red Blood Cell as a Model*, Wiley-VCH, Weinheim, **2003**.
- [11] Numerous papers are being published on the influence of Li^+ ions on many biochemical and pathobiochemical processes owing to its high positive-charge density, but a complete picture of the medicinal and biochemical properties of Li^+ is not yet available. In any case, Li^+ ions play a key role in the treatment of bipolar disorder (manic depression), the mechanism of which is not known; for examples, see: H. R. Pilcher, *Nature* **2003**, *425*, 118; S. J. Lippard, J. M. Berg, *Bioinorganische Chemie, Spektrum, Heidelberg*, **1995**; *Principles of Bioinorganic Chemistry*, University Science Books, Mill Valley, USA, **1994**. It has been reported that Li^+ ions block the recycling pathway for inositol-1,4,5-triphosphate (IP_3); malfunctions of the inositol system have been linked to a number of illnesses, including manic depression and cancer; see: G. Thomas, *Medicinal Chemistry: An Introduction*, Wiley, Chichester, **2000**.
- [12] Preliminary experiments directed towards competition in the uptake/release of Li^+ and Na^+ ions show that for $c(Li^+) = 30$ mM and $c(Na^+) = 15$ mM (in the form of NaBr), almost all of the “capsule-bound” Li^+ ions are replaced by Na^+ ions; that is, about 98% of the Li^+ ions are present in the form of $[Li(dms)_n]^+$ (signal I), whereas about 70% of the Na^+ are bound to the capsule ($\delta(^{23}Na) = -1.5$ and -12 ppm ($W_{1/2} = 2.6$ kHz) for $[Na(dms)_n]^+$ and Na^+C2a , respectively). This is a remarkable result that shows the relatively high affinity of the capsule for Na^+ as they block/close the pores/channels^[6b] (different aspect in ref. [6]).

Corrigendum

In this Communication, the temperature assignments on the right-hand side of Figure 4 were incorrect. The Editorial Office apologises for this error. The correct figure is shown.



Artificial Cells: Temperature-Dependent, Reversible Li⁺-Ion Uptake/Release Equilibrium at Metal Oxide Nanocontainer Pores**

A. Müller,* D. Rehder,* E. T. K. Haupt,
A. Merca, H. Bögge, M. Schmidtman,
G. Heinze-Brückner _____ **4466–4470**

Angew. Chem. Int. Ed. **2004**, *43*

DOI 10.1002/anie.200453762



On the complex hedgehog-shaped cluster species containing 368 Mo atoms: simple preparation method, new spectral details and information about the unique formation

Achim Müller^{*}, Bogdan Botar, Samar K. Das, Hartmut Bögge, Marc Schmidtman, Alice Merca

Faculty of Chemistry, University of Bielefeld, P.O. Box 100131, 33501 Bielefeld, Germany

Received 21 June 2004; accepted 26 July 2004

Available online 11 September 2004

Abstract

The deep-blue compound $\text{Na}_{48}[\text{H}_x\text{Mo}_{368}\text{O}_{1032}(\text{H}_2\text{O})_{240}(\text{SO}_4)_{48}] \cdot \text{ca. } 1000\text{H}_2\text{O} \equiv \text{Na}_{48} \mathbf{1a} \cdot \text{ca. } 1000\text{H}_2\text{O} (\mathbf{1})$ exhibiting an unusual nanosized hedgehog-type cluster anion, could now be obtained in good yield – allowing now several materials science studies – in the presence of a high concentration of an electrolyte destroying the hydration shell, in only two days. $\mathbf{1}$ was characterized by elemental analysis (including redox titrations to determine the (formal) number of Mo^{V} centers), thermogravimetry and spectroscopic methods (IR, resonance Raman, Vis/NIR). Information about unusual aspects of the formation is reported together with additional spectroscopic details as well as a new crystal structure determination of the very complex system while confirming the earlier one. © 2004 Elsevier Ltd. All rights reserved.

Keywords: Clusters; Complexity; Nanochemistry; Polyoxomolybdates

1. Introduction

Aesthetically beautiful giant polyoxomolybdates of the type $\{\text{Mo}_{11}\}_n$ which are either sphere- ($n = 12$) or wheel-shaped ($n = 14$) can now be obtained by undergraduates in facile syntheses [1,2]. Following our related work other research groups have also reported comparable syntheses of the cluster species [3] and used them e.g., for materials science studies (see below). The mentioned cluster anions, in spite of their completely different overall structure, have formally similar building blocks resulting in the remarkable mentioned equivalent stoichiometry [2e] which is also of importance for the

cluster reported here. The related molybdate building units abundant in a unique ‘dynamic library’ can form – via a type of ‘split and/or link process’ – a versatility of molecular architectures upon slight variation of the boundary conditions under reduced conditions. This is especially the case for Mo-blue-type solutions [2] from which the above mentioned wheel-type species can be obtained. From this ‘library’ an even larger and highly reduced cluster anion containing 368 Mo atoms can – under very special conditions – be obtained [4] which shows much more structural complexity than the wheel-type cluster species. As the related earlier published synthetic method requires a rather long time – crystallization occurs only after 2 weeks according to the high solubility – we report here (1) a facile synthesis allowing now several types of studies together with some detailed spectroscopic information for an easy identification of the cluster, (2) a second (crystal) structure

^{*} Corresponding author. Tel.: +49 521 106 6153; fax: +49 521 106 6003.

E-mail address: a.mueller@uni-bielefeld.de (A. Müller).

determination for the extremely complex inorganic cluster confirming the earlier published one and (3) further details about the related cluster-formation problem which seems to be interesting.

2. Experimental

The chemicals were purchased from commercial sources and all manipulations were performed using materials as received.

2.1. $Na_{48}[H_xMo_{368}O_{1032}(H_2O)_{240}(SO_4)_{48}] \cdot ca. 1000 H_2O$, $x \approx 16$

To a solution of 6 g $Na_2MoO_4 \cdot 2H_2O$ (24.8 mmol) in 25 ml of water acidified with 100 ml 0.5 M H_2SO_4 , 0.18 g $N_2H_6SO_4$ (1.38 mmol) as reducing agent is added under stirring. After stirring for 30 min 1.50 g NaCl (25.6 mmol) is added. The solution is then stored in a closed flask for 2 days and the precipitated deep-blue crystals of **1** are filtered off. Yield: 1.2 g (23% based on Mo). Characteristic IR bands (KBr pellet, cm^{-1}): $\nu = 1620m$ ($\delta(H_2O)$), 1199w, 1101w, 1060 (all $\nu_{as}(SO_4)$), 981/958s ($\nu(Mo=O)$), 765s, $\approx 700sh$, 628w, 557m, 462w; characteristic resonance Raman bands (solid/KBr dilution, $\lambda_e = 1064$ nm, cm^{-1}): $\nu = 810m$, 681w, 456 m; Vis spectrum (in H_2O , nm): $\lambda = 785$ (very broad) ($\epsilon = 2.4 \times 10^5$ $mol^{-1} dm^3 cm^{-1}$). *Elemental Anal.* Calc.: Na, 1.39; S, 1.92. Found: Na, 1.5; S, 2.2% (cerimetric titration ≈ 110 Mo^V centers).

Vibrational spectra were recorded on a Bruker FTIR IFS 66 with a Raman FRA 106 unit spectrophotometer

($\lambda_e = 1064$ nm). The Vis spectrum was measured using a Shimadzu UV-3101PC instrument.

3. Results and discussion

By reducing an aqueous molybdate solution acidified with sulfuric acid – the important reagent in the present case, corresponding to [4] – the deep-blue giant mixed-valence cluster anion **1a** (Fig. 1) with the size of hemoglobin is formed and can be crystallized as Na salt. In order to improve the yield of the synthesis and decrease the crystallization time we changed the reaction conditions leading to a decrease of the solubility of **1** due to the presence of a rather high concentration of an electrolyte, which destroys the hydration shell of the giant cluster anion (see Section 2). The presence of the hydration shell caused by the abundance of a large number of H_2O ligands – which are responsible for the high solubility of molybdenum blue type species – prevented the isolation of crystalline Mo-blue type materials for more than 200 years since the times of Scheele and Berzelius [2], see also [5–7].

Compound **1**, which was now obtained with a facile synthesis by decreasing the solubility drastically, was characterized by elemental analysis (including redox titrations to determine the (formal) number of Mo^V centers), thermogravimetry (to determine the actual crystal water content which is important for the analyses), and spectroscopic methods (IR, resonance Raman, Vis/NIR). The data obtained for the new synthesized compound agree with those of the earlier reported substance including the results of the thermogravimetry [4].

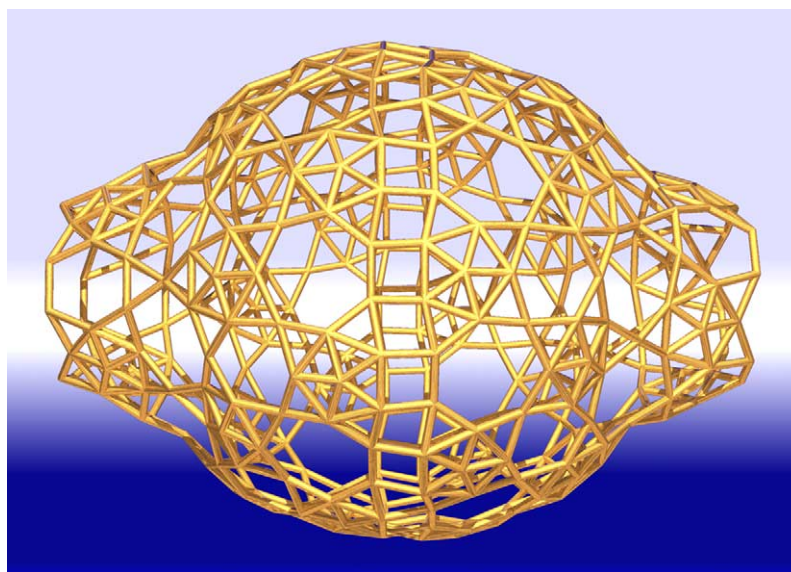


Fig. 1. $\{Mo_{368}\}$ metal atom framework of **1a** in wire-frame representation showing nicely the change from positive via negative to positive curvature at the surface.

$\text{Na}_{48}[\text{H}_x\text{Mo}_{368}\text{O}_{1032}(\text{H}_2\text{O})_{240}(\text{SO}_4)_{48}] \cdot \text{ca. } 1000\text{H}_2\text{O} \equiv \text{Na}_{48}$
1a $\cdot \text{ca. } 1000\text{H}_2\text{O}$ (**1**). **1a** $\equiv [\text{H}_x\{(\text{Mo})\text{Mo}_5\}'_8\{(\text{Mo})\text{Mo}_5\}''_{32}$
 $\{\text{Mo}_2\}'_{16}\{\text{Mo}_2\}''_8\{\text{Mo}_2\}'''_8\{\text{Mo}_1\}_{64}]^{48-}$ ($x \approx 16$ correspond-
 ing to $\approx 112 \text{ Mo}^{\text{V}}$ -type centers).

Definitions: $\{(\text{Mo})\text{Mo}_5\}' \equiv \{\text{Mo}_6\text{O}_{21}(\text{H}_2\text{O})_6\}$; $\{(\text{Mo})\text{Mo}_5\}''$
 $\equiv \{\text{Mo}_6\text{O}_{21}(\text{H}_2\text{O})_3(\text{SO}_4)\}$; $\{\text{Mo}_2\}' \equiv \{\text{Mo}_2\text{O}_3(\text{H}_2\text{O})_2\}$;
 $\{\text{Mo}_2\}'' \equiv \{\text{Mo}_2\text{O}(\text{t})_2\text{O}(\text{br})_3(\text{SO}_4)\}$; $\{\text{Mo}_2\}''' \equiv \{\text{Mo}_2\text{O}(\text{t})_4$
 $\text{O}(\text{br})(\text{SO}_4)\}$; $\{\text{Mo}_1\} \equiv \{\text{MoO}(\text{H}_2\text{O})\}$.

Compound **1** crystallizes in the space group *I4mm* and contains in the unit cell two giant hedgehog-like cluster anions **1a** with a central spheroid-shaped fragment $\{\text{Mo}_{288}\text{O}_{784}(\text{H}_2\text{O})_{192}(\text{SO}_4)_{32}\} = \text{B}$ and two capping units $\{\text{Mo}_{40}\text{O}_{124}(\text{H}_2\text{O})_{24}(\text{SO}_4)_8\} = \text{C}$ (note: the second structure analysis which confirmed the earlier published one was performed with crystals obtained with the earlier reported synthesis [4]). Remarkably, there are three rather large areas, i.e. $2\text{C} + \text{B}$, with different local symmetries: D_{8d} in the central **B** part and C_{4v} in the two capping areas **C**. There is a small error limit for the correlated number of protonations and Mo^{V} centers.

The comparably large number of different building units of **1a** can be identified from the above given formulae. The two $\{(\text{Mo})\text{Mo}_5\}$ -type units differ with respect to the abundance of the SO_4^{2-} ligands (32 occur with SO_4^{2-} ligands, and 8 without, located in the C_{4v} areas; the two numbers were erroneously referred to in [4]). The dinuclear units $\{\text{Mo}_2\}$ do not only differ with respect to the abundance of bidentate SO_4^{2-} ligands (see formulae): those at the ends of both **C** caps, i.e., the borderlines, have contrary to the other type two terminal O atoms at both Mo centers, a situation characteristic for stopping growth. The $\{\text{Mo}_1\}$ units are of the 'classical' type $\{\text{OMo}^{\text{V}}(\text{H}_2\text{O})\}^{3+}$ and contribute correspondingly to the highly reduced state of **1a**; the remaining predominantly Mo^{V} -type centers are distributed over several parts of the large cluster areas and cause a widespread delocalization of Mo (4d) electrons while the capping units **C** are less reduced (corresponding the size of the cluster and the resolution obtained there are of course limits with respect to the interpretation of the bond valence sum values). This again causes broad peaks in the resonance Raman and electron absorption spectra of **1**. The structure of the cluster anion can be formally considered as a hybrid between the $\{\text{Mo}_{176}\}/\{\text{Mo}_{154}\}$ -type giant molecular wheels and the $\{\text{Mo}_{102}\}/\{\text{Mo}_{132}\}$ -type spherical clusters mentioned above (for details see [4]).

The high reduction state (ca. $112 \text{ Mo}^{\text{V}}/256 \text{ Mo}^{\text{VI}}$), which is much higher than that in the above mentioned Mo-blue type wheel systems (i.e. $28 \text{ Mo}^{\text{V}}/126 \text{ Mo}^{\text{VI}}$ for $n = 14$ [2a]), refers to the fact that strong reducing conditions favour cluster growth (see [4]). The largest cluster existing in acidified molybdate solution is – in absence of a reducing agent – the 'rather small' $\{\text{Mo}_{36}\}$ anion [2,8,9] which 'starts growing' upon reduction [2a].

Due to the rather short crystallization time of the new synthesis method no suitable crystals for single crystal X-ray diffraction analysis were obtained. Important in this context is that in case of less symmetrical giant species like **1a** nucleus formation is less favoured than in case of more symmetrical and smaller ones (see [10]). A crystal obtained according to the earlier reported synthetic method was again used for a new crystal structure determination. As even the crystals of the latter method are normally obtained in small size, data were collected with an instrument equipped with a rotating anode and an X-ray mirror (see Acknowledgements). The structure analysis confirmed the earlier reported one.¹ Compound **1**, obtained with the new method, could be identified clearly by comparison of the spectroscopic (Figs. 2 and 3) and analytical data with those of the earlier reported compound obtained with the synthesis leading to larger crystals [4]. Especially the IR spectrum of **1** (Fig. 2) is very characteristic and, e.g., different from the compounds containing the other Mo-blue-type species, i.e., the wheel-shaped clusters [1b], and can therefore be easily used for the simple identification. The presence of the bidentate SO_4^{2-} ligands is proven by the IR bands at 1199, 1101, 1060 cm^{-1} originating from the $\nu_3(F_2)$ vibration of discrete SO_4^{2-} .

Some important additional experiments have to be mentioned. If K^+ ions are present in the reaction mixture not the hedgehog-type species is formed but a derivative of the $\{\text{Mo}_{176}\}$ wheel-type cluster in which a novel $\{\text{KSO}_4\}_{16}$ ring has been integrated [11]. The related unusual species was reported recently in a paper [11] entitled 'Synergetic activation of 'silent receptor' sites leading to a new type of inclusion complex: integration of a 64-membered ring comprising K^+ and SO_4^{2-} ions into a molybdenum oxide-based nanoobject'. The unusual inclusion species $[\text{Mo}_{114}^{\text{VI}}\text{Mo}_{32}^{\text{V}}\text{O}_{429}(\text{H}_2\text{O})_{50}(\text{KSO}_4)_{16}]^{30-}$ shows the remarkable 64-membered $\{\text{K}(\text{SO}_4)\}_{16}$ ring integrated into a wheel-shaped nanocluster host. It is formed by a novel unprecedented reaction type, based on synergetically induced functional complementarity [11]. Furthermore it represents a text-book example of a very complex non-biological material. The K^+ ions have in presence of SO_4^{2-} a direct influence on the activation of the ring-type cluster's silent receptor sites and prevent formation of the $\{\text{Mo}_{368}\}$ -type cluster having much smaller formation tendency than the more

¹ The structure of **1** was redetermined using crystals prepared according to the earlier reported method [4]. The lattice constants were determined as $a = 43.257(2)$, $c = 68.999(5)$ Å, $V = 129111(13)$ Å³. The structure could be nicely refined in space group *I4mm* as done in [4], though the situation showed that the partial 'disorder' of a part of the anion could be removed by refining the structure in space group *I4* assuming that the crystal is merohedrally twinned. The special twin problem will be considered separately at a later date.

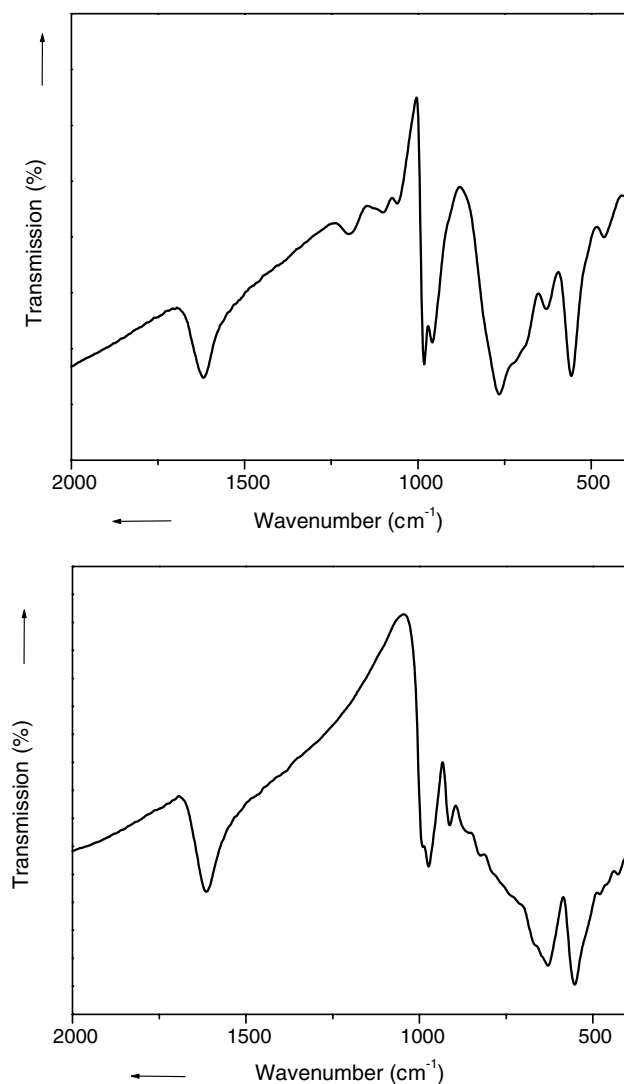


Fig. 2. IR-spectra of **1** (KBr pellets; top) and of the typical wheel-shaped Mo-blue cluster $\{\text{Mo}_{154}\}$ (bottom, see [1b], too). (See Section 2 for details.)

symmetrical one. On the other hand in the presence of Li^+ cations in the reaction mixture also not the hedgehog-type species is formed but the neutral spherical $\{\text{Mo}_{102}\}$ ball-type cluster species [12]. The results can be understood, as the wheel- and ball-shaped species have a much higher formation tendency while the formation of the very complex $\{\text{Mo}_{368}\}$ cluster, showing in case of the synthesis of **1** an unprecedented symmetry breaking of the surface, really only occurs under very special limited conditions. Note: the role of the Na^+ cations is not understood until now.

The knowledge of the cluster **1a** will probably be the starting point for the syntheses of related other clusters of comparable size. This should be possible in case of the abundance of ligands like ‘the medium-ligand-strength’ SO_4^{2-} ions generating a large number of building units (for details see [4]) and may be a starting point of an interesting route in nanochemistry. This includes also

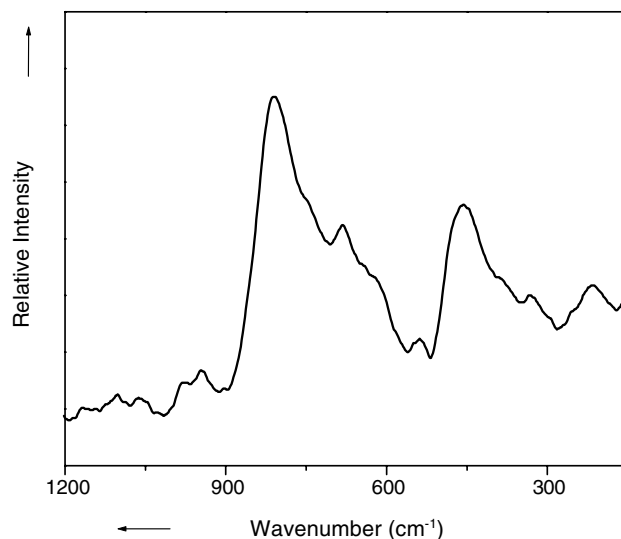


Fig. 3. Solid state resonance-Raman spectrum of **1**. The missing intense lines due to $\nu(\text{Mo}=\text{O})$ vibrations proves that the corresponding terminal bonds are not involved in the Mo 4d electron delocalization as compared to the $\{\text{Mo}_{154}\}$ wheel-type species, where in each of the 14 $\{\text{Mo}_5\text{O}_6\}$ units two 4d electrons are delocalized (see [2a]). (See Section 2 for experimental details.)

the option of handling the giant clusters as intact units for instance for the preparation of composites, e.g., with silica or cationic surfactants, which is possible with these types of anionic clusters as was shown before in case of the above mentioned giant ball- and wheel-type species with the generation of micelles, films, monolayers and even liquid crystals [13]. A further option for the future is to study the vesicle formation of the giant cluster which follows unprecedented principles (see [14]).

An important result of the present paper is the formation of an extreme complex structure, showing symmetry breaking at the surface which is very much dependent on the special synthesis conditions in contrary to cases of higher symmetrical species (see [15]).

Acknowledgements

The authors thank Prof. G.M. Sheldrick for collecting data for a single-crystal X-ray structure analysis under the mentioned special conditions. The financial support from the Fonds der Chemischen Industrie, the Deutsche Forschungsgemeinschaft, the Volkswagen Stiftung and the European Union (Brussels) is highly acknowledged. S.K. Das thanks the Alexander von Humboldt-Foundation and A. Merca the ‘Graduiertenkolleg Strukturbildungsprozesse’, Universität Bielefeld, for their fellowships.

References

- [1] (a) L. Cronin, E. Diemann, A. Müller, in: J.D. Woollins (Ed.), *Inorganic Experiments*, Wiley-VCH, Weinheim, 2003, p. 340;

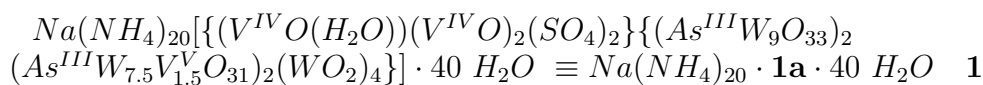
- (b) A. Müller, S.K. Das, E. Krickemeyer, C. Kuhlmann, in: J. Shapley (Ed.), *Inorg. Synth.*, vol. 34, Wiley, New York, 2004, p. 191.
- [2] (a) A. Müller, C. Serain, *Acc. Chem. Res.* 33 (2000) 2;
(b) A. Müller, P. Kögerler, C. Kuhlmann, *Chem. Commun.* (1999) 1347;
(c) A. Müller, S. Roy, *Coord. Chem. Rev.* 245 (2003) 153;
(d) N. Hall, *Chem. Commun.* (2003) 803;
(e) A. Müller, P. Kögerler, H. Bögge, *Struct. Bond. (Berlin)* 96 (2000) 203.
- [3] (a) T. Yamase, P.V. Prokop, *Angew. Chem., Int. Ed.* 41 (2002) 466;
(b) K. Eda, Y. Sato, Y. Iriki, *Chem. Lett.* (2002) 952;
(c) C. Jiang, Y. Wei, Q. Liu, S. Zhang, M. Shao, Y. Tang, *Chem. Commun.* (1998) 1937;
(d) W. Yang, C. Lu, X. Lin, S. Wang, H. Zhuang, *Inorg. Chem. Commun.* 4 (2001) 245.
- [4] A. Müller, E. Beckmann, H. Bögge, M. Schmidtman, A. Dress, *Angew. Chem., Int. Ed.* 41 (2002) 1162.
- [5] *Gmelins Handbuch der anorganischen Chemie*, vol. 53 (Mo), Verlag Chemie, Berlin, 1935, pp. 134–147.
- [6] *Gmelin Handbook of Inorganic Chemistry*, vol. B3a, Mo Suppl., Springer-Verlag, Berlin, 1987, pp. 63–65.
- [7] *Gmelin Handbook of Inorganic Chemistry*, vol. B3b, Mo Suppl., Springer-Verlag, Berlin, 1989, pp. 15–16.
- [8] M.T. Pope, A. Müller, *Angew. Chem., Int. Ed.* 30 (1991) 34.
- [9] When it was published it was considered as the largest (!) inorganic anion: K.H. Tytko, B. Schönfeld, B. Buss, O. Glemser, *Angew. Chem. Int. Ed. Engl.* 12 (1973) 330.
- [10] A. Müller, E. Diemann, B. Hollmann, H. Ratajczak, *Naturwissenschaften* 83 (1996) 321.
- [11] A. Müller, L. Toma, H. Bögge, M. Schmidtman, P. Kögerler, *Chem. Commun.* (2003) 2000.
- [12] A. Müller, S.-Q. Nazir-Shah, H. Bögge, M. Schmidtman, P. Kögerler, B. Hauptfleisch, S. Leiding, K. Wittler, *Angew. Chem., Int. Ed.* 39 (2000) 1614.
- [13] (a) S. Polarz, B. Smarsly, C. Göltner, M. Antonietti, *Adv. Mater.* 12 (2000) 1503;
(b) S. Polarz, B. Smarsly, M. Antonietti, *Chem. Phys. Chem.* 2 (2001) 457;
(c) D. Kurth, P. Lehmann, D. Volkmer, A. Müller, D. Schwahn, *J. Chem. Soc., Dalton Trans.* (2000) 3989 (and relevant literature cited therein);
(d) Yan Zhu, A. Cammers-Goodwin, B. Zhao, A. Dozier, E.C. Dickey, *Chem. Eur. J.* 10 (2004) 2421.
- [14] T. Liu, E. Diemann, H. Li, A.W.M. Dress, A. Müller, *Nature* 426 (2003) 59.
- [15] A. Müller, S.K. Das, H. Bögge, M. Schmidtman, A. Botar, *Chem. Comm.* (2001) 657.

Chapter 3

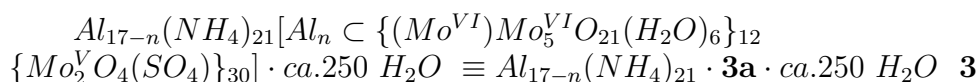
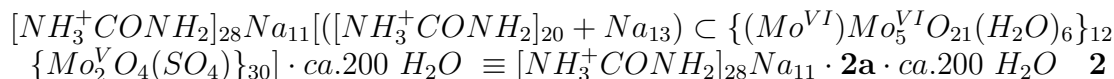
Summary

Since the discovery of the crown ethers supramolecular chemistry has been dealing with molecular containers. Over the decades, the flat crown ethers have given way to three-dimensional shapes including cryptands, cavitands and ultimately capsules, designed to encapsulate molecular hosts¹. Now the emphasis is shifting from structure to function, as researchers are trying to make the nanoscale capsules work for them. This is possible through the absolutely unique class of polyoxometalates. In solutions of oxoanions of the early transition metals - in particular molybdates and tungstates - an enormous variety of compounds can be formed by linking together metal-oxide building blocks. In this dissertation we investigated the host-potential of some polyoxometalates and their formation stability.

The $\{As_4M_{40}O_{140}\}$ -type cryptand **1a** exhibits a new type of reactive internal cavity shell, which allows interesting "encapsulation chemistry" positioning a variety of cationic as well as anionic "guests" under confined conditions according to a new approach: Replacement of some of the W by V atoms leads to higher reactivity of the internal cavity shell as a result of relatively weak VO bonds compared to the WO situation which allows the encapsulation of two sulphate groups replacing O atoms of the $\{AsM_9\}$ units.

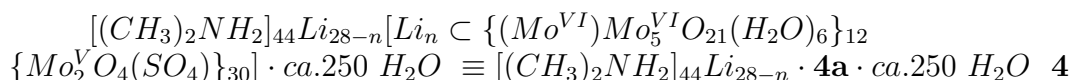


Looking at the host-functionalities of the $\{Mo_{132}\}$ type spherical clusters, different substrates/cations can be fixed at well-defined positions above, below, and especially in the channels. In this sense the clusters **2a** and **3a** were synthesised.



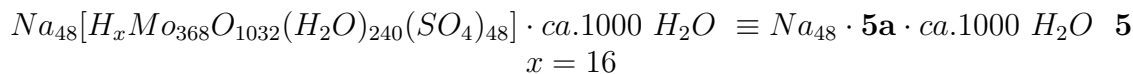
¹M. Gross, *Chemistry in Britain* **2003**, Aug. Issue, p. 18.

As shown earlier this situation allows to study, new types of ion transport phenomena, on the nanoscale, and shows properties of a "nano-ion chromatograph". Additionally, one can construct new geometric solids from entering cations owing to the fact that we have a multitude of different as well as equivalent sites in the channels, pores, and in the interior mentioned only in the science papers. The stable and soluble spherical molybdenum oxide based porous nanocontainer interacts with the Li^+ cations abundant in solution and incorporates them at well-defined internal positions obtaining compound **4**.



Even though the presence of the Li^+ cations inside the cavity could not be proven by single crystal X-ray structure analysis because of the relevant disorder, the coordination inside the cavity is to some extent supported by infrared spectroscopy. The traffic of Li^+ ions between the outside and inside of the capsule is in equilibrium as measured by 7Li NMR spectroscopy.

The importance of the presence of the "suitable" cations for the assembly of (large) polyoxometalate structures, revealed the investigations on the formation of compound **5**.



In the presence of Li^+ , K^+ or NH_4^+ cations in the reaction mixture, not the lemon-type species is formed but the wheel- and ball-shaped species, which have a much higher formation tendency.

Chapter 4

Curriculum Vitae

Alice Merca
Schulstraße 57
33647 Bielefeld
Deutschland
Tel: +49-521-1362304
Email: *merca_alice@yahoo.com*

PERSONALS

Born on 9th Feb., 1978 in Huedin, Romania, married, Romanian nationality

PROFESSIONAL EXPERIENCE

11/2001 - present Doctoral student, University of Bielefeld, Germany, Faculty of Chemistry, supervisor: Prof. Dr. Dr. h. c. mult. Achim Müller

EDUCATION

07/2001 Licentiate in Chemistry, topic of the thesis: Synthese, Eigenschaften und Struktur eines neues Polyoxowolframates mit Bismut (III) als Heteroatom, supervisor: Conf. Dr. Adrian Patrut

10/1997 - 06/2001 Student of the "Babes-Bolyai" University, Cluj-Napoca, Romania, Faculty of Chemistry and Chemical Engineering, specialization: Chemistry - Physics; german section

09/1992 - 07/1996 "Gheorghe Sincai" National Colleg, Baia-Mare, Romania

HONORS

11/2001 - 10/2004 Fellowship granted by the Graduiertenkolleg "Strukturbildungsprozesse", University of Bielefeld, Germany

03/1997 - 06/2001 Studentship granted by the "Babes-Bolyai" University Cluj-Napoca, Romania

COMPUTER SKILLS

Windows 3.x/95/98/Me/2000,
Microsoft Office (Word, Excel, PowerPoint), Origin, Corel Draw, Internet related software

LANGUAGES

Fluent German and Hungarien, Intermediate English, Basic French, Romanian (mother language)

LIST OF PUBLICATIONS

1. A. Müller, S. K. Das, S. Talismanov, S. Roy, E. Beckmann, H. Bögge, M. Schmidtman, A. Merca, A. Berkle, L. Allouche, Y. Zhou, L. Zhang, **"Trapping cations in specific positions in tuneable "artificial cell" channels: new nanochemistry perspectives."** *Angew. Chem. Int. Ed.* **2003**, *42*, 5039-5044.

2. A. Müller, D. Rehder, E.T.K. Haupt, A. Merca, H. Bögge, M. Schmidtman, G. Heinze-Brückner, **"Temperature-dependent reversible Li^+ uptake/release equilibrium at metal-oxide nanocontainer-pores."** *Angew. Chem. Int. Ed.* **2004**, *43*, 4466-4470; Corrigendum: *43*, 5115.

3. A. Müller, B. Botar, S. K. Das, H. Bögge, M. Schmidtman, A. Merca, **"On the complex hedgehog shaped cluster species containing 368 Mo atoms: simple preparation method, new spectral details and information about the unique formation."** *Polyhedron* **2004**, *23*, 2381-2385.

4. A. Müller, M. T. Pope, A. Merca, H. Bögge, M. Schmidtman, J. van Slageren, M. Dressel, D. G. Kurth, **"A small cavity with reactive internal shell atoms spanned by four $\{As(W/V)_9\}$ -type building blocks allows host guest chemistry under confined conditions."** *Chem. Eur. J.* **2005**, accepted.

5. A. Müller, A. Merca, H. Bögge, M. Schmidtman, A. Berkle, **"Artificial cell decision about metal cations entrance: the "stable" aqua complexes get trapped above the pores others slip out its water coat and the cations enter."** *Chem. Commun.* **2005**, to be submitted.

6. A. Müller, L. Toma, H. Bögge, A. Merca, S. Roy, A. Stammler, **"Twenty "corks" gating-opening porous capsules: related solution uptake-release equilibrium allows cation uptake."** *Angew. Chem. Int. Ed.* **2005**, to be submitted.

7. A. Müller, S. Roy, A. Merca, H. Bögge, M. Schmidtman, **"Linking wheel-shaped giant polyoxomolybdates to chains."** in preparation.